

"Photovoltaic effect and quadratic electro-optic modulation in specific iodine-doped nonconjugated conductive polymers"

by

Sumeeth Jaju

A thesis submitted to the Graduate Faculty of
Auburn University
in partial fulfillment of the
requirements for the Degree of
Master of Science

Auburn, Alabama
December 13th, 2014

Keywords: Nonconjugated conductive polymer, Cis-1,4-polyisoprene, Photovoltaic Effect, Quadratic electro-optic effect, Modulation depth

Copyright 2014 by Sumeeth Jaju

Approved by

Mrinal Thakur, Chair, Professor of Mechanical Engineering
Lloyd S. Riggs, Co-chair, Professor of Electrical and computer Engineering
Dan Marghitu, Professor of Mechanical Engineering

Abstract

In this thesis, photovoltaic effect and quadratic electro-optic modulation in specific iodine-doped nonconjugated conductive polymers (NCP) have been reported. Exceptionally large quadratic electro-optic effects in specific iodine-doped nonconjugated conductive polymers have been previously reported. In the present work, an intensive research has been undertaken in order to enhance the electro-optic modulation-depth for the electro-optic device applications. Quadratic electro-optic modulation has been measured at 633nm using field-induced birefringence method. Photovoltaic cells involving specific iodine-doped nonconjugated conductive polymers have been fabricated and enhanced photo-voltages and photocurrents have been measured.

Iodine-doped nonconjugated conductive polymers such as poly(β -pinene), cis-1,4-poly(isoprene) and styrene-butadiene-rubber (SBR) upon doping with iodine were used to fabricate photovoltaic cells. The cells formed using SBR polymer did not show as much voltage and current compared to the other two polymers. Photovoltaic cells have been fabricated using titanium dioxide/doped NCP/carbon on ITO glass-substrates. Photocurrents and photo-voltages for different intensities of light (from a white illuminant light bulb, emission at 300-700 nm) have been measured. Use of iodine-doped nonconjugated conductive polymer film has led to

significant enhancement of photocurrent compared to previous reports involving undoped polymer-C₆₀ composites in a different structure.

A maximum photocurrent of about 0.3 mA was observed for a light intensity of ~ 5 mW/cm² and maximum photo-voltage (open-circuit) was about 0.6 V for the photovoltaic cell fabricated using doped poly(β -pinene) whereas the maximum photocurrent of about 0.25 mA and maximum photo-voltage (open-circuit) was about 0.75 V for the same light intensity for photovoltaic cell fabricated using cis-1,4-poly(isoprene).

Quadratic electro-optic modulation in iodine-doped cis-1,4-poly(isoprene) has been measured at the wavelength of 633nm using field-induced birefringence method. A modulation depth of about 5% has been observed at 633nm at an applied field of ~ 1 V/ μ m for about 50 μ m thick film. The modulation depth had a quadratic dependence on applied field. Enhanced modulation has also been observed in a optical fiber waveguide coated with iodine-doped nonconjugated conductive polymer. The Kerr coefficients measured are exceptionally large and have been attributed to the subnanometer size metallic domains (quantum dots) formed upon doping and charge-transfer.

Acknowledgements

I take this opportunity to thank my academic advisor Dr. Mrinal Thakur, for his guidance in my research throughout my Master's degree program here in Auburn. I am obliged to Dr. Lloyd Riggs and Dr. Dan Marghitu for serving on my advisory committee.

I wish to extended my appreciation to my colleagues Mradul Sangal, Justin at Photonics Materials Research Laboratory for their help throughout my research work. I also like to thank all my friends who have been helpful throughout my degree.

I wish to dedicate this degree and work to my family who made this possible and for all their support throughout my life.

Table of Contents

Abstract.....	ii
Acknowledgements.....	iv
List of Figures.....	viii
Chapter 1 INTRODUCTION.....	1
Chapter 2 OBJECTIVES.....	4
Chapter 3 BACKGROUND.....	6
3.1 Governing Maxwell’s Equation.....	6
3.2 Interaction of light in an optical medium.....	7
3.2.1 Isotropic medium.....	7
3.2.2 Anisotropic medium.....	8
3.3 Linear and Nonlinear Optical Processes.....	10
3.3.1 Linear optical process.....	10
3.3.2 Nonlinear optical process.....	10
3.4 Nonlinear optical materials.....	17
3.4.1 Second order Optical Material.....	18
3.4.2 Third Order Optical Materials.....	18
3.5 Photovoltaic cells.....	19
3.5.1 Differentiating Organic Photovoltaic cells (OPV) to Inorganic Photovoltaic cells (IPV)	20
3.6 Quadratic Electro-optic effect.....	24

Chapter 4 NONCONJUGATED CONDUCTIVE POLYMERS	28
4.1 Poly (β -pinene) (PBP)	29
4.2 Polyisoprene	30
4.2.1 Cis-1,4-polyisoprene (CPI).....	31
4.2.2 Trans-1,4-polyisoprene (TPI)	32
4.3 Styrene-butadiene-rubber (SBR).....	33
Chapter 5 PHOTOVOLTAIC CELLS INVOLVING NONCONJUGATED CONDUCTIVE POLYMER IODINE-DOPED POLY(β -PINENE).....	35
5.1 Introduction	35
5.2 Experiment	38
5.3 Results and Discussion:.....	41
5.4 Conclusion.....	43
Chapter 6 PHOTOVOLTAIC CELLS INVOLVING NONCONJUGATED CONDUCTIVE POLYMER IODINE-DOPED CIS-1,4-POLY(ISOPRENE).....	44
6.1 Introduction	44
6.2 Experiment	44
6.3 Results and Discussion.....	47
6.4 Conclusion.....	49
Chapter 7 QUADRATIC ELECTRO-OPTIC EFFECT OF NONCONJUGATED CONDUCTIVE POLYMER 1,4-CIS-POLYISOPRENE	51
7.1 Introduction	51
7.2 Optical Absorption	52
7.3 Sample preparation for Electro-optic experiment	53
7.4 Experimental setup.....	54
7.4.1 Results	55
7.5 Experimental Setup for Guided Wave	55
7.5.1 Results	56

7.6 Conclusion.....	57
Chapter 8 SUMMARY	58
Bibliography	60

List of Figures

Figure 3.1 Sum of Frequency Generation.....	12
Figure 3.2 Difference of Frequency Generation	13
Figure 3.3 Second-harmonic Generation	14
Figure 3.4 Energy level diagrams for different second order nonlinear processes	15
Figure 3.5 Basic Photovoltaic cell experimental setup	20
Figure 3.6 Binding energy compared with distance separating the electron and origin generated hole.....	21
Figure 3.7 Schematic diagrams showing the effect of charge carrier distribution.....	22
Figure 3.8 Photocurrent density with voltage for two cells	23
Figure 3.9 Recombination rates with distance for short circuit	24
Figure 4.1 Molecular structure of Poly(β -pinene)	29
Figure 4.2 Undoped Polyisoprene.....	30
Figure 4.3 Schematic of the intersite hopping transport in a doped nonconjugated conductive polymer (polyisoprene)	30
Figure 4.4 The electrical conductivities for cis- and trans- polyisoprene lie on the solid curve and the data for poly (dimethylbutadiene) lie on the dashed curve. From Reference 2 (Macromolecules 1988)...	31
Figure 4.5 Molecular structure of Cis-1,4-polyisoprene.....	31
Figure 4.6 Absorption Spectra of CPI at different doping level with iodine	32
Figure 4.7 Molecular structure of Trans-1, 4- polyisoprene	33
Figure 4.8 Molecular structure of styrene-butadiene-rubber.	34
Figure 5.1 World Population statistics.....	35
Figure 5.2 World Energy Consumption from 1980-2030.....	36

Figure 5.3 World energy consumption by energy source	37
Figure 5.4 Molecular structure of poly(β -pinene) before and after iodine-doping	39
Figure 5.5 Optical absorption spectra of poly(β -pinene) for different doping levels of iodine. The heavily doped samples as used here correspond to iodine molar concentration of about 0.8.....	39
Figure 5.6 Experimental set-up for photo-voltaic measurements. The inset shows the emission spectrum of the light source used in the experiment	40
Figure 5.7 Measured photocurrent for different light intensities. The area of the device was $\sim 5 \text{ cm}^2$	42
Figure 5.8 Measured photo-voltages for different light intensities. For dark condition the measured voltage was about 50 mV	42
Figure 6.1: Molecular structure of Cis-polyisoprene	45
Figure 6.2 Molecular structure of cis-1,4-poly(isoprene) after iodine-doping	45
Figure 6.3 Optical absorption spectra of cis-1,4-poly(isoprene) for different doping levels of iodine. The heavily doped samples as used here correspond to iodine molar concentration of about 0.65	46
Figure 6.4 Experimental set-up for photo-voltaic measurements. The inset shows the emission spectrum of the light source used in the experiment	47
Figure 6.5 Measured photocurrent for different light intensities. The area of the device was $\sim 5 \text{ cm}^2$	48
Figure 6.6 Measured photo-voltages for different light intensities. For dark condition the measured voltage was about 40 mV	49
Figure 6.7 A schematic of the mechanism involved in the photovoltaic effect in these cells.....	49
Figure 7.1 Transformation of double bond into cation radicals.....	51
Figure 7.2 Optical absorption spectra of 1,4 cis-polyisoprene at different doping levels. y-molar concentration of iodine.....	52
Figure 7.3: Experimental setup for electro-optics.....	53
Figure 7.4: Experimental setup for Guided wave Electro-optics.....	55
Figure 7.5 Quadratic modulation depth due to the applied Electric field.....	56

Chapter 1

INTRODUCTION

The science and technology that deal with applications of light (photons) is known as Photonics. It blends together optics and electronics to effectively handle and process enormous amount of data with exceptional speed. It has wide range of applications that include emission, transmission, signal processing, modulation etc. using light. Studies of linear and nonlinear optical properties of materials build the core of such applications in photonics. Novel nanomaterials and structures provide immense scope to the field of photonic applications. This present thesis deals with the study of such new nonconjugated conductive polymers.

With the increase in demand for energy and the depletion of nonrenewable sources of energy, trend has been shifting towards the use of renewable sources. Renewable source device such as Solar cells or photovoltaic cells are used as fuel, which convert incident light energy into electrical energy. These solar cells use either inorganic materials or organic materials for this conversion. Inorganic materials have been main ingredient of solar cells for few decades, but its fabrication process is complicated and installation is costly. To overcome these disadvantages scientists started working on organic materials for their applications in solar cells. Nonconjugated conductive polymers discussed in this thesis may provide significantly lower cost alternatives to inorganic and other organic system for photovoltaics.

Exceptionally large third order optical susceptibility have been recently reported for nonconjugated conductive polymers (organic nanometallic materials). The largest known two photon absorption coefficients and quadratic electro-optic effect have been measured in specific

iodine doped nonconjugated conductive polymers since. Low dielectric constant and electronic nonlinearity make these polymers highly promising for ultrafast optic signal processing. In this research enhancement of electro-optic modulation depth has been explored so that advancement towards such application is made.

Nonconjugated conductive polymers are a great discovery in the photonics, electronic and telecommunication fields besides applications in protection against nuclear radiation. Their low dielectric constants ensure that the speed is never compromised. Further ease of fabrications and the flexibility they provide to the engineer at the molecular level has made these materials particularly important. It would not be surprising if these materials soon become the backbone of the various related fields. To validate this more evidences are provided by our research which is divided into following areas:

1. Photovoltaic cells involving nonconjugated conductive polymer, poly(β -pinene) (PBP).
2. Photovoltaic cells involving nonconjugated conductive polymer, cis-1,4-poly(isoprene) (CPI).
3. Quadratic electro-optic effect of nonconjugated conductive co-polymer cis-1,4-poly(isoprene) , doped with iodine at shorter wavelength .
4. Enhancement of electro-optic modulation depth.

These works are systematically organized in different chapters. The overall goals of this research and studies are discussed in Chapter 2, titled as Objective. The basic theories and fundamental concepts of photonics and nonlinear optics that support this thesis are briefly discussed as Background in Chapter 3. In Chapter 4 we will discuss about various nonconjugated conductive polymers and its molecular structure and electrical properties.

In Chapter 5, a review of the world energy needs and the different sources of energy are discussed. A brief idea of the present world energy consumption and the projected needs is discussed. Then the process of fabrication of a photovoltaic cell using a composite involving nonconjugated conductive polymer, poly(β -pinene) (PBP) upon doping with iodine has been discussed.

In Chapter 6, process of fabrication of a photovoltaic cell using a composite involving nonconjugated conductive polymer, cis-1,4-poly(isoprene) (CPI) upon doping with iodine has been discussed.

In Chapter 7, discussion about the quadratic electro-optic effect in the nonconjugated conductive co-polymer iodine-doped cis-1,4-poly(isoprene) measured at specific wavelengths.

In Chapter 8, brief summary of the whole research has been mentioned along with the future work.

Chapter 2

OBJECTIVES

Photovoltaic is one of the areas which can cater to the increasing demand of energy. Solar energy is the most abundantly available renewable energy source. An attempt to use this energy by converting it into photovoltage using technology involving ease and low cost has been the driving force behind this research carried out here. As reported earlier, the quadratic electro-optic coefficients in specific nonconjugated conductive polymers are the largest known for any material. Therefore, the other major objective is to make advancements toward utilization of these unusual electro-optic properties in modulation/switching applications. The polymers to be studied in this research will include: poly(β -pinene) (PBP), cis-1,4-polyisoprene (CPI), trans-1,4-polyisoprene (TPI) and a copolymer styrene-butadiene-rubber (SBR).

Extensive research has been carried out on photovoltaics using conjugated conductive polymers. The aim of the present research is to fabricate photovoltaic cells using a nonconjugated conductive polymer and to improve the results by altering the sample structures. The quadratic electro-optic effect in iodine-doped cis-1,4-polyisoprene polymer will be studied using field-induced birefringence technique under different device-configurations.

The specific objectives of this research are:

- Fabrication of films of specific nonconjugated conductive polymers with controlled thickness
- Characterization of the nonconjugated conductive polymer films before and after doping with iodine
- Fabrication of photovoltaic cells using these films

- To analyze photo-voltaic characteristics of these cells
- To analyze the dependence of the photovoltage produced on the intensity of the light source used
- To analyze the dependence of the photovoltage produced on the amount of time the composite was doped in iodine
- To analyze the photovoltaic characteristics of other nonconjugated conductive polymers such as poly(β -pinene) and styrene-butadiene rubber (SBR)
- To study the quadratic electro-optic effect in doped polymer films
- Use the doped polymer films in waveguide and other configurations to enhance electro-optic modulation-depth for electro-optic device applications

Chapter 3

BACKGROUND

Nonlinear optics represents one of the most recent advancements in Photonics. It is the study of phenomena that occurs due to modification of the optical properties of a medium in the presence of an electric field or an intense laser light. Optical nonlinearity occurs when a material system gives a nonlinear response with applied fields. The effects may include: frequency conversion, linear and quadratic electro-optic modulation/switching, all-optical modulation, optical limiting and others [8-11].

3.1 Governing Maxwell's Equation

The propagation of light is governed by few fundamental equations known as Maxwell's equations. Light is an electromagnetic wave for which the direction of propagation and the electric and magnetic fields are mutually perpendicular to each other. The Maxwell's equations for electric and magnetic field vectors \vec{E} and \vec{H} , and \vec{B} and \vec{D} as electric and magnetic displacement vectors, have the following differential forms. [36, 38]

$$\nabla \cdot \vec{D} = \rho \quad \text{Eqn. (3.1)}$$

$$\nabla \cdot \vec{B} = 0 \quad \text{Eqn. (3.2)}$$

$$\nabla \times \vec{E} = -\frac{\partial \vec{B}}{\partial t} \quad \text{Eqn. (3.3)}$$

$$\nabla \times \vec{H} = \mathbf{J} + \frac{\partial \vec{D}}{\partial t} \quad \text{Eqn. (3.4)}$$

ρ and \mathbf{J} are electric charge and current densities. In optics, for most cases, one deals with negligible electrical or thermal conductivity referred as dielectric. With dielectrics media, there is no free charge and no current flow, therefore ρ and \mathbf{J} are zero.

Distortion of atomic orbitals has been described by polarization magnetization, caused by electromagnetic field. Conductivity is defined by the flow of electric charges. The following relations hold. [3, 4-6]

$$\vec{B} = \mu_0 (\vec{H} + \vec{M}) \quad \text{Eqn. (3.5)}$$

$$\vec{J} = \sigma \vec{E} \quad \text{Eqn. (3.6)}$$

$$\vec{D} = \epsilon_0 \vec{E} + \vec{P} \quad \text{Eqn. (3.7)}$$

Where ϵ_0 = vacuum permittivity (dielectric constant)
 μ_0 = Vacuum permeability
 P = Induced polarization due to applied electric field
 M = Induced magnetization due to applied magnetic field

3.2 Interaction of light in an optical medium

Optical media can be classified into two types:

1. Isotropic medium
2. Anisotropic medium

3.2.1 Isotropic medium

The term ‘isotropy’ refers to having similar properties for all direction in a medium. The electric field \vec{E} , displacement vector \vec{D} and polarization \vec{P} do not depend on the direction of electric field in an isotropic medium. The polarization induced is always parallel to applied electric field; it always carries a linear relationship. Thus linear polarization for an isotropic medium is expressed by the following equation.

$$\vec{P} = \epsilon_0 \chi \vec{E} \quad \text{Eqn. (3.8)}$$

Correspondingly, the relationship between the displacement vector and susceptibility is given by

$$\vec{D} = \epsilon_0 (1 + \chi) \vec{E} \quad \text{Eqn. (3.9)}$$

In an isotropic medium electrons are tightly bound to the nucleus, which makes these materials non-conducting and nonmagnetic. As a result these materials can be compared to the dielectric medium when subjected to an external electric field. The polarization due to the dipole, induced by the electric field is mention below [9].

$$P = -Ner \quad \text{Eqn. (3.10)}$$

Where P is the polarization, e is the electronic charge, and r is the displacement induced by the electric field. Correspondingly the wave equation for such a medium can be stated as

$$\nabla \times \nabla \times \vec{E} = \nabla \times \left(-\frac{\partial \vec{B}}{\partial t} \right) \quad \text{Eqn. (3.11)}$$

The final wave equation derived as

$$\nabla \times \nabla \times \vec{E} + \frac{1}{c^2} \frac{d^2 E}{dt^2} = -\mu_0 \frac{d^2 P}{dt^2} - \mu_0 \frac{dJ}{dt} \quad \text{Eqn. (3.12)}$$

3.2.2 Anisotropic medium

The term ‘anisotropy’ refers to different properties for different directions in a media. In this directionally dependent nonlinear medium, the polarization is not necessarily parallel to the applied electric field. And hence the polarization P can be expressed by the following equations given below.

$$P_1 = \epsilon_0 (\chi_{11} E_1 + \chi_{12} E_2 + \chi_{13} E_3) \quad \text{Eqn. (3.13)}$$

$$P_2 = \epsilon_0 (\chi_{21} E_1 + \chi_{22} E_2 + \chi_{23} E_3) \quad \text{Eqn. (3.14)}$$

$$P_3 = \varepsilon_0(\chi_{31}E_1 + \chi_{32}E_2 + \chi_{33}E_3) \quad \text{Eqn. (3.14)}$$

Where χ the susceptibility is a tensor of rank 2 and the electric displacement vector D is given by

$$D_i = \varepsilon_i(1 + \chi_{ij}) E_i = \varepsilon_{ij}E_j \quad \text{Eqn. (3.15)}$$

Where ε_{ij} represents the permittivity tensor. If a co-ordinate system is chosen such that it coincides with the principal dielectric axes of the medium, we get the following matrix:

$$\begin{bmatrix} D_x \\ D_y \\ D_z \end{bmatrix} = \begin{bmatrix} \varepsilon_x & 0 & 0 \\ 0 & \varepsilon_y & 0 \\ 0 & 0 & \varepsilon_z \end{bmatrix} \begin{bmatrix} E_x \\ E_y \\ E_z \end{bmatrix}$$

The energy density due to the electric field is given by

$$U = \frac{1}{2} D \cdot E \quad \text{Eqn. (3.16)}$$

Since the x, y, z are chosen along the principal axes, we have

$$U = \frac{1}{2} [\varepsilon_{11}E_1^2 + \varepsilon_{22}E_2^2 + \varepsilon_{33}E_3^2] \quad \text{Eqn. (3.17)}$$

$$2U = \frac{D_1^2}{\varepsilon_{11}} + \frac{D_2^2}{\varepsilon_{22}} + \frac{D_3^2}{\varepsilon_{33}}$$

$$\text{If } x = D_1\sqrt{2U}, y = D_2\sqrt{2U}, z = D_3\sqrt{2U}$$

$$\frac{x^2}{n_x^2} + \frac{y^2}{n_y^2} + \frac{z^2}{n_z^2} = 1 \quad \text{Eqn. (3.18)}$$

Equation (3.18) is known as optical indicatrix equation, it shows the relationship between the refractive index and the direction of polarization in a nonlinear anisotropic medium[7,12,13].

Since the indicatrix equation traces the path of an ellipsoid, it is also referred to as refractive index ellipsoid.

3.3 Linear and Nonlinear Optical Processes

Optical materials can be classified into two categories

1. Materials with predominantly linear optical properties
2. Materials with second, third or higher order optical nonlinearities

3.3.1 Linear optical process

In an isotropic dielectric media, polarization occur due to applied electric field, while in anisotropic media it may not be. The electric field and linear polarization are expressed as

$$\vec{E}(\vec{r}, t) = \vec{E}_0 \exp(\vec{k} \cdot \vec{r} - \omega \cdot t) + c. c \quad \text{Eqn. (3.19)}$$

$$\vec{P} = \epsilon_0 \chi^{(1)} \vec{E}$$

And the real dielectric constant is expressed as

$$\epsilon = 1 + \chi^{(1)} = \left\{ n + i\alpha \frac{c}{2\omega} \right\}^2 \quad \text{Eqn. (3.20)}$$

Where n is refractive index, α is absorption coefficient and $\chi^{(1)}$ is linear susceptibilities.

3.3.2 Nonlinear optical process

Earlier studies show that the advent of lasers linear relationship did not hold good. Then a nonlinear dependence of polarization with applied electric field was reported [12-15]. Nonlinear optical media, the propagation of light is not so simple. The polarization depends on higher powers of electric field and is usually highly anisotropic.

$$\vec{P} = \varepsilon_0(\chi^{(1)}\vec{E}(t) + \chi^{(2)}\vec{E}^2(t) + \chi^{(3)}\vec{E}^3(t) + \chi^{(4)}\vec{E}^4(t) + \dots) \quad \text{Eqn. (3.21)}$$

$$\vec{P} = \overrightarrow{P^{(1)}}(t) + \overrightarrow{P^{(2)}}(t) + \overrightarrow{P^{(3)}}(t) + \dots$$

Where $\chi^{(2)}$ and $\chi^{(3)}$ are second and third order susceptibilities, after truncating linear part of series, $\vec{P}^{(1)} = \chi^{(1)}\vec{E}(t)$, the rest of the series is known as nonlinear polarization.

$$\overrightarrow{P_{NL}} = \varepsilon_0(\chi^{(2)}\vec{E}^2(t) + \chi^{(3)}\vec{E}^3(t) + \chi^{(4)}\vec{E}^4(t) + \chi^{(5)}\vec{E}^5(t) + \dots) \quad \text{Eqn. (3.22)}$$

3.3.2.1 Second order nonlinear processes

Nonlinear optical materials can be classified as centrosymmetric and non-centrosymmetric. Centrosymmetric materials are those materials in which polarization is an odd function of electric field. Since $P(-E) = -P(E)$ holds well in centrosymmetric materials, the even terms are zero. In centrosymmetric materials

$$\chi^{(2)}E_2 = -\chi^{(2)}E_2 \quad \text{Eqn. (3.23)}$$

This is possible only when $\chi^{(2)} = 0$ or $\chi^{(2n)} = 0$ for all positive integers of n.

Whereas non-centrosymmetric materials are those materials in which polarization is an even function of electric field. Since $P(-E)$ is not equal to $P(E)$ in non-centrosymmetric materials, the even terms can be nonzero. Clearly it is seen that the optical material should be non-centrosymmetric to exhibit second order nonlinear properties.

There are various outcomes when photons interacted with a nonlinear optical medium. These are as follows.

1. Sum frequency generation, Second harmonic generation
2. Difference frequency generation
3. Third harmonic generation
4. Optical rectification

These depend on experimental, or device configuration and the effect is larger for materials with higher nonlinearities.

3.3.2.1.1 Sum-Frequency Generation

Sum frequency generation is a nonlinear optical process used to study the molecular structure and dynamics at the surface and interfaces. When in a strong applied field, two laser beams having strong frequency ω_1 and a weak applied field frequency ω_2 interact with nonlinear material; there is a situation in which the strong signal ω_1 , combine with the weak signal ω_2 to produced higher frequency signal $\omega_3 = \omega_1 + \omega_2$ [16].

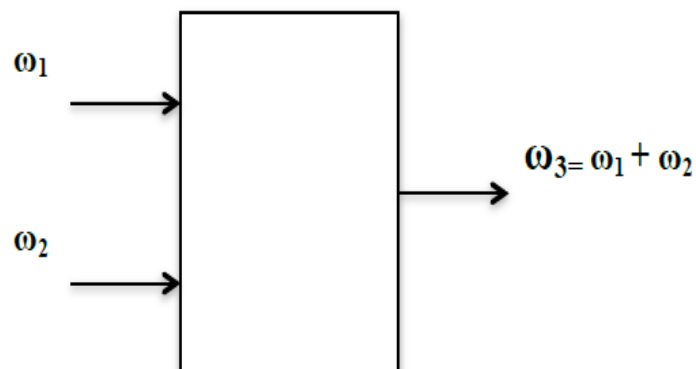


Figure 3.1 Sum of Frequency Generation

3.3.2.1.2 Difference-Frequency Generation

In this process, applied input fields with input frequencies ω_1 or ω_2 and ω_3 interact with nonlinear medium to produce output frequency as the difference between the other two frequencies. This process is similar to sum of frequency process. However in this processes, applied input fields (with frequencies ω_1 or ω_2 and ω_3) interact with lossless nonlinear material to produce an output signal at difference frequency ($\omega_2 = \omega_3 - \omega_1$) or ($\omega_1 = \omega_3 - \omega_2$).

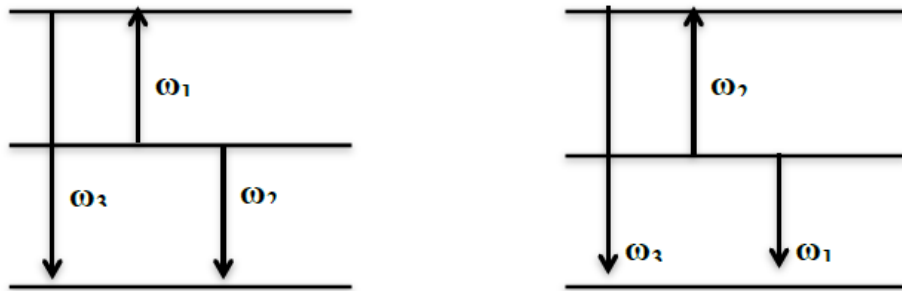


Figure 3.2 Difference of Frequency Generation

3.3.2.1.3 Second harmonic Generation

Second harmonic generation (SHG) is also known as frequency doubling. It is a nonlinear optical process in which photons interact with a nonlinear material, merging effectively to form new photons with twice the energy, and therefore twice the frequency and half the wavelength of the input photons. Second harmonic generation is regarded as a special case of sum frequency generation. Full permutation symmetry of susceptibilities have been seen in second harmonic generation which are primarily caused by two fundamental frequencies ω_1 and $\omega_2 = 2\omega_1$. The $\omega_2 = 2\omega_1$ is the second harmonic frequency/frequency doubling frequency as shown in Figure 3.3

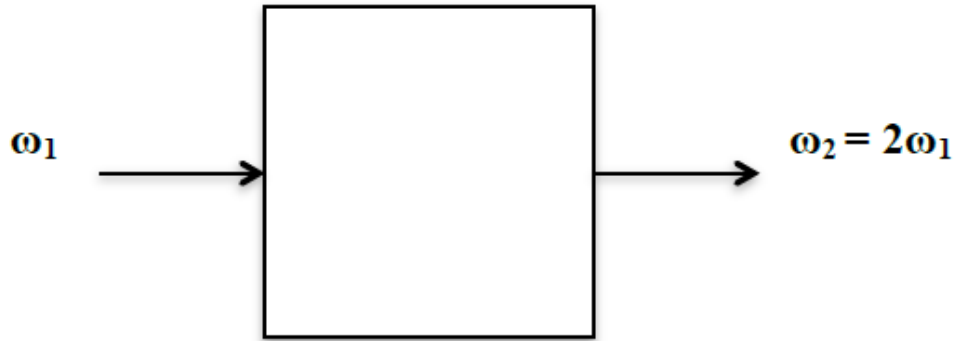


Figure 3.3 Second-harmonic Generation

3.3.2.1.4 Third Harmonic Generation

Third Harmonic Generation is also known as optical frequency multiplier. An optical frequency multiplier is a nonlinear optical device, in which photons interact with a nonlinear material, and merge effectively to form new photons with greater energy, producing higher frequency and shorter wavelength. Direct third harmonic generation (THG), also called frequency tripling) exists, and can be used to discover the interface between materials of different excitability. It is widely used in high power lasers and inertial confinement fusion experiments.

3.3.2.1.5 Optical Rectification

Nonlinear second order susceptibility is the main cause of nonlinear optical processes. There is a different case with two equal frequencies, in second order susceptibility given as in Eqn.(3.24)

$$\chi_{kij}^{(2)}(0, \omega, -\omega) = \chi_{jki}^{(2)}(0, \omega, \omega) \quad \text{Eqn. (3.24)}$$

It consists of one real part and one imaginary part. The real part of $\chi_{jki}^{(2)}(0, \omega, \omega)$ defines Pockels effect or linear electro-optics. When an optical beam and a dc (or low frequency ac) electric field interact with a second order material, there is change in refractive index observed proportional to applied dc electric field. This process is known as **Pockel's effect** or **linear electro-optic effect**. This was first observed by a German physicist Friedrich Pockel in 1906 [17,18]. Where else the real part of $\chi_{kij}^{(2)}(0, \omega, -\omega)$ define another process known as optical rectification. When two electric fields interact with each other in nonlinear medium results in a static electric field then the process is called optical rectification [19].

The energy level diagram for the above three processes is shown in the figure below.

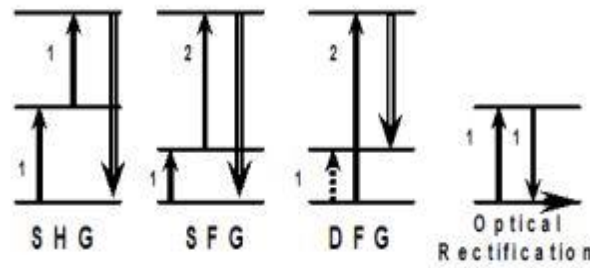


Figure 3.4 Energy level diagrams for different second order nonlinear processes

3.3.2.2 Third order nonlinear processes

Third order nonlinear processes are based on the term $\epsilon_0(\chi^{(3)}\vec{E}^3)$ in the polarization expansion of the Eqn. (3.21). The most general third order process nonlinear process involves the interaction of four different frequencies: $\omega_1, \omega_2, \omega_3,$ and ω_4 . The ω_1, ω_2 and ω_3 are distinct frequencies for third order polarization in NLO materials and is given by the equation:

$$E(t) = E_1(t)e^{-i\omega_1 t} + E_2(t)e^{-i\omega_2 t} + E_3(t)e^{-i\omega_3 t} + c.c$$

When some of these materials interact with an optical field and a slow time varying external field, the change in the indices $[\chi^{(3)}(\omega = \omega + 0 + 0)]$ is quadratically related to the external field applied. This effect is denoted as **Kerr effect**. This effect was first reported by a Scottish physicist John Kerr in 1875 [20]. Kerr effect can be observed when a laser beam propagates through a third order material. Kerr effect is the change in the refractive index of a material in response to an applied electric field and is given by the equation below

$$\Delta n = k\lambda E^2 \quad \text{Eqn. (3.25)}$$

Where Δn = change in refractive index,

K = Kerr co-efficient,

λ = wavelength of the laser beam and

E = magnitude of the slow time varying electric field.

$$\Delta n = n_2 I \quad \text{Eqn. (3.26)}$$

Where n_2 is the nonlinear refractive index and I is the intensity of the laser source.

The nonlinear refractive index is related to the third order susceptibility χ^3 as per the equation below.

$$n_2 = \frac{12\pi^2 \chi^3}{c^2 n_0} \quad \text{Eqn. (3.27)}$$

Where n_0 is weak field refractive index of the material and c is the speed of light.

When a laser source whose transverse intensity propagates through a nonlinear material, a phase delay due to Kerr effect deforms the wave front causing it to either focus or defocus depending on the sign of the nonlinear refractive index n_2 [17]. If n_2 is negative the material behaves like a negative lens which diverge the beam and is called self-defocusing. When n_2 the material behaves like a positive lens, it converges the incident beam is known as self-focusing.

3.4 Nonlinear optical materials

The field of nonlinear optics has witnessed exponential growth after the advent of laser since 1960. Nonlinear materials interact with high intensity light to produce nonlinear effect. Based on the composition, these materials can be primarily be categorized into two classes organic and inorganic [21]. Inorganic NLO materials such as lithium niobate (LiNbO_3) or potassium dihydrogen phosphate (KH_2PO_4) are known to exhibit second harmonic generation (SHG) effect [22]. As a result during the last 40 year these inorganic materials have been seen dominating the world of nonlinear optics. Where else as far as organic materials are concerned, during the 1990's, p-electron organic materials were identified as promising candidates for nonlinear optical applications. However, more recent studies of NLO materials have focused on the use of organic materials with π -electron conjugated systems [23]. Such materials offer the advantages of larger optical nonlinearity and faster optical response. Other driving forces behind the recent development of organic NLO's include higher bandwidth, lower driving voltage, more flexible device design, and potentially lower processing cost [24]. In this section we will discuss about various orders of nonlinear optical materials.

3.4.1 Second order Optical Material

In early 1960s development and characterization of nonlinear material was done on some criteria. These criteria includes the material must be non-centrosymmetric, must have excellent optical quality and high refractive index, must easily available etc. The first reported nonlinearity was observed in quartz when Franklin and co-workers recorded a very weak second harmonic signal in quartz using Q-switched ruby laser source [25]. In 1962 two research teams individually showed that phase matching in ammonium-dihydrogen phosphate (ADP) can result in significantly stronger second harmonic signals [26,27]. Two years later Boyd and co-workers reported lithium meta-niobate (LiNbO₃) to be “An efficient phase matchable NLO material.”[28] Further inquiries in LiNbO₃ showed some advantages and disadvantages, but the despite this shortcoming this material is perhaps the most popular inorganic NLO material. Later several investigators presented the application of organic nonlinear material in various fields i.e. photovoltaic, photonic devices etc.

However these researchers reported the potential of organic materials in photonic devices much attention was given to inorganic materials in 1960s [29, 30]. This trend changed when Kutz demonstrated a powder technique to evaluate the optical nonlinearities in powder samples of materials. The shift in focus on organic nonlinear materials was due to the several advantages they have over their inorganic counterparts. Since NLO effects are electronic in nature, exceptionally high switching speeds can be attained [31].

3.4.2 Third Order Optical Materials

A wide range of materials have been invested for third order nonlinearities since for these materials did not require symmetry condition. Different techniques such as third harmonic

generation (THG), degenerate four-wave mixing (DFWM) and self-focusing techniques were used to determine third order susceptibility. However due to variability of the nature of experimental conditions used in the optical processes, it was difficult to compare the results initially. However the ongoing research from several years has made it possible to develop materials that have high third order. One such developed third order material is nonconjugated conducting polymers. A particular discussion has been done on nonconjugated conducting polymers in next chapter(4).

3.5 Photovoltaic cells

Photovoltaic is the branch of science that deals with the conversion of light energy to electrical energy. Modern day photovoltaic (PV) cells can be divided into two broad categories **inorganic** and **organic**. An inorganic PV cell normally acts like a PN junction. When light strikes the junction, electron hole pairs are created; electrons flow to the positive side and holes flow to the negative side and this constitutes a flow of current. The driving forces in this process are the built-in potential and the work functions of the contacts. In organic PV cells a different mechanism is used. They consist of composite involving a polymer and an electron acceptor. Light of appropriate wavelength excites the electrons in the polymer and these electrons are accepted by the electron acceptor and are carried through a low work function electrode while the holes are carried through an electrode that has a higher work function.

The first functional photovoltaic cell was fabricated in 1883 by Fritts [32]. He used Selenium to fabricate the cell. The basic structure of a photovoltaic cell is as shown.

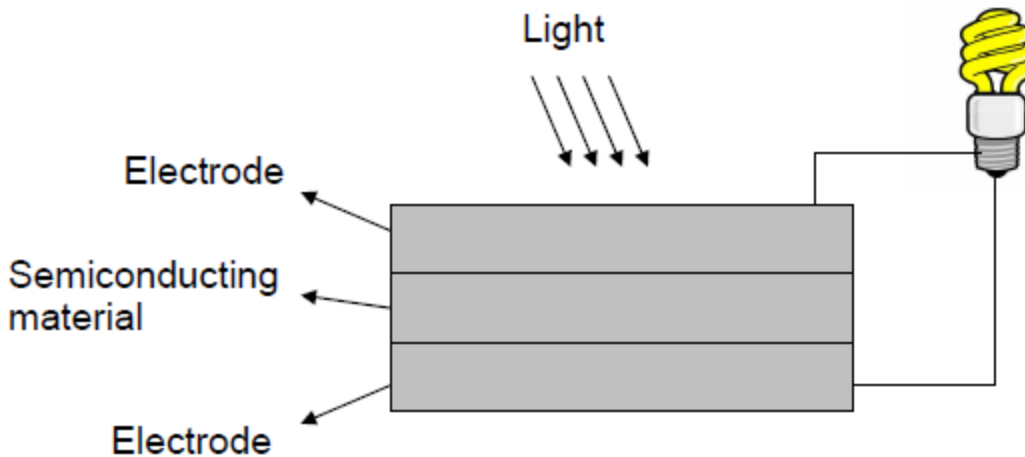


Figure 3.5 Basic Photovoltaic cell experimental setup

Most of the photovoltaic cells used thin films to obtain high efficiency. To obtain larger amount of power, the photovoltaic cells are connected in series to form a grid. Efforts are being made to further increase the efficiency of the cells. Majority of the photovoltaic cells in the market use silicon. Due to the increase in demand for the photovoltaic cells, the price of Silicon has risen in the recent years. This mainly resulted in significant research in the area of photovoltaics using organic conductive polymers. Conductive polymers are those having a special structure which becomes conductive upon doping with an electron acceptor.

3.5.1 Differentiating Organic Photovoltaic cells (OPV) to Inorganic Photovoltaic cells (IPV)

- The fundamental difference between solar cells made using organic materials and inorganic photovoltaic cells is that the light absorption results in the formation of

excitons (bound state of electron and hole pair with Coulomb force) in molecular materials rather than free electrons and holes.

- The dielectric constant of organic materials is usually low compared to that of inorganic materials resulting in attractive Coulomb potential well around charges.
- In organic materials, non-covalent electronic interactions (narrow bandwidth) between the molecules are weak compared to strong covalent interatomic electronic interactions in inorganic materials like silicon.
- The above two points are reasons for the formation of excitons in organic materials rather than free electrons and holes which are created throughout the bulk when light is absorbed.

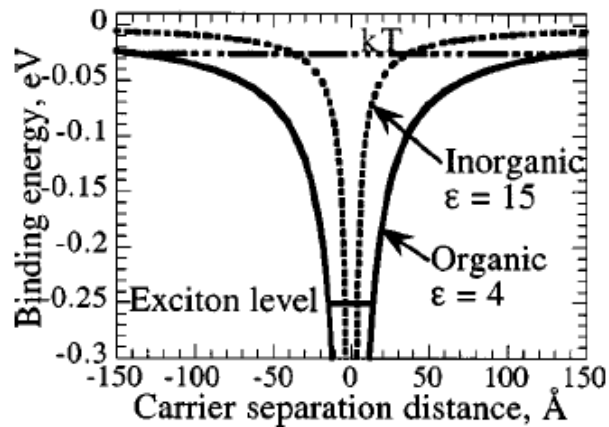


Figure 3.6 Binding energy compared with distance separating the electron and origin generated hole [34]

- Because of low equilibrium carrier densities, OPV under illumination are always majority carrier devices unlike most IPV cells which are minority carrier devices.
- The energy of excitons (optical band gap) is less than the free electron-hole pair (electrical band gap), the difference between the exciton binding energy.

- For an efficient collection of photons, the absorption spectrum of the material layer must match the solar emission spectrum and the layer should be sufficient thick to absorb most of the light. The optical absorption coefficient (α) of organic materials is much higher than that of inorganic material silicon in crystalline or multicrystalline form.
- And the thickness of the silicon layer must be twice the thickness of the organic layer to reduce the light intensity.
- Light absorption in IPV cells results in production of electrons and holes in same material. As the two carriers have the same spatial distribution and concentration gradient, the carrier types are driven in same direction. Since this is small driving force in IPV cells the electrical potential gradient present at p-n junction is able to separate the carrier types effectively. But in the case of OPV cells excitons are produced which requires a large potential gradient that drives the charge carriers away from the interface.

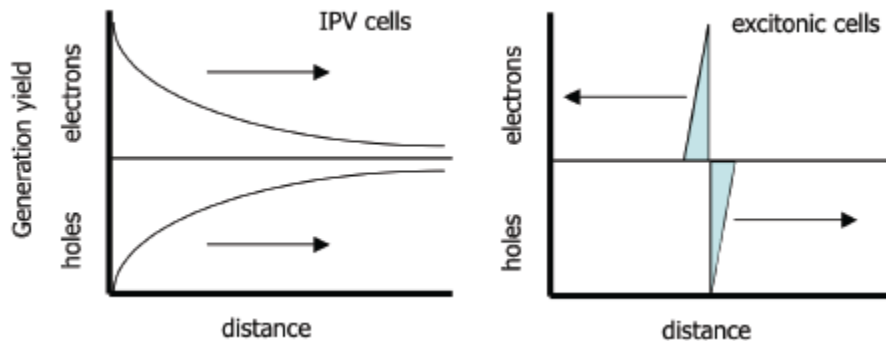


Figure 3.7 Schematic diagrams showing the effect of charge carrier distribution [33]

- The mobility in organic materials ($< 0.1\text{cm}^2/\text{Vs}$) is relatively small compared to the inorganic materials ($100\text{-}10000\text{cm}^2/\text{Vs}$).

- Electric field is main driving force for charge transport in IPV cells whereas it is not yet clear to what extent that the internal electric field contributes to charge transport in the OPV cells.
- For OPV cells the open circuit voltage (V_{oc}) values obtained are reasonable compared to the IPV cells where V_{oc} is limited by the electrostatic potential at the junction.

$$V_{oc} = \text{Ionization potential of p-type material} - \text{Electron affinity of n-type layer}$$
- The OPV cell generates a much stronger Photovoltaic effect compared to that of IPV cell because the charge carriers are generated only at the heterointerface and they are already separated across the phase boundary.

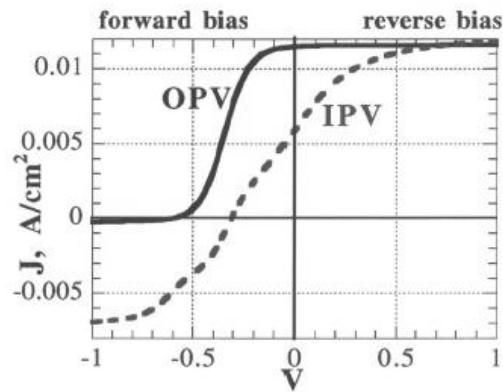


Figure 3.8 Photocurrent density with voltage for two cells [34]

- After charge generation mechanism, recombination in the IPV cell occurs mainly in the bulk while recombination in the OPV cell occurs mostly at the interface.
- Bulk properties are important for IPV cells because carriers are photogenerated and also recombine in bulk whereas it happens in interfacial region and hence its properties are important for the OPV cells.

- Optimizing bulk properties such as crystallinity in IPV cell and optimizing interfacial properties such as maximizing exciton dissociation rate in OPV cell are key performances in minimizing the recombination rates.

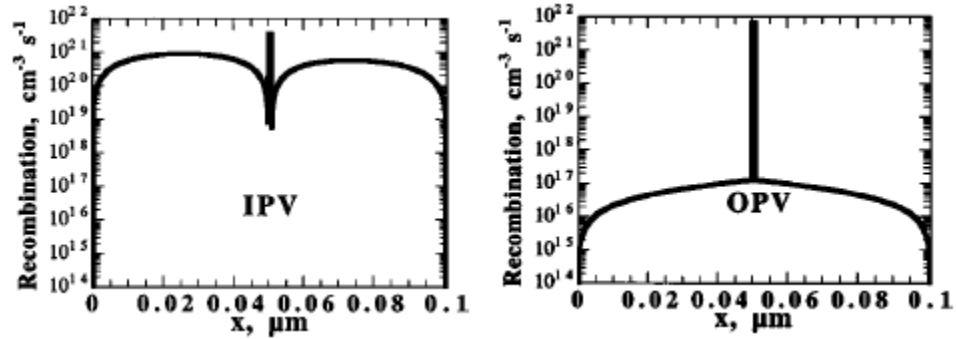


Figure 3.9 Recombination rates with distance for short circuit [34]

- The spatial location of photogenerated charge carriers results in fundamental changes in photovoltaic behavior with others held constant. This mechanism mostly distinguishes IPV cells from OPV cells.
- OPV cells have certain disadvantages including their low efficiency (only 5%) and short lifetime whereas IPV cells have efficiency of 20 % and better lifetime.
- But OPV cells are compatible with flexible substrates and have low cost high throughput printing techniques compared to IPV cells which are expensive, heavy, rigid and not yet compatible with real low cost technology.

3.6 Quadratic Electro-optic effect

The electro-optics effect refers to the change in refractive index due to the applied electric field. If the change is linear to the applied electric field it is called linear electro optic effect. In this case the induced polarization of the material is linearly proportional to the electric field and is also termed as **Pockels effect**. Crystal having centered of symmetry show no linear

electro-optics effect. There is induced index change that is directly proportional to the square of the electric field instead of varying linearly with it. In other words induced polarization in the material is quadratically proportional to the applied electric field. Such effect is also referred as Quadratic electro-optics effect or **Kerr effect**. This interaction of the optical radiation with the material subjected to an electric field can be described completely in terms of the impermeability tensor η_{ij} by the relation [35]

$$\vec{E}_i = \sum_j \eta_{ij} \vec{D}_j \quad \text{Eqn. (3.28)}$$

Quantum theory of solids, dictates that the optical dielectric impermeability tensor depends on the distribution of charges in the crystal. When an electric field is applied, redistribution of the bound charges occur and also possibly a slight deformation of the ion lattice causing a change in the optical impermeability tensor. This change in the impermeability tensor can be related to the applied electric field by the following relation

$$\Delta\eta_{ij} = r_{ijk}E_k + s_{ijkl}E_kE_l \quad \text{Eqn. (3.29)}$$

Where, r_{ijk} is the linear electro-optic coefficient as described in section 3.2 and s_{ijkl} is the quadratic electro-optic coefficient. The s_{ijkl} coefficient varies as the square of the applied electric field therefore it's called the quadratic electro-optic effect which was first discovered by J. Kerr in 1875 in optically isotropic media such as glasses and liquids. Unlike linear electro-optic effect which is observed in anisotropic media, the quadratic electro-optic effect is seen in all media and there are no symmetry restrictions. In noncentrosymmetric media the linear electro-optic effect is more predominant than the quadratic effect. But in centrosymmetric media it's the prominent nonlinearity. When an electric field is applied, the dimensions and orientation of the index ellipsoid change depending on the direction of the applied electric field and also on the symmetry properties of the 6×6 matrix elements of the s_{ijkl} coefficient. In an optically

isotropic media such as polymers, the application of electric field makes the media birefringent which mainly depends on the alignment of the molecules affected by the electric field. The media then behaves as a uniaxial medium where the direction of the applied electric field defines the optical axis. Usually, the z-axis is chosen to be the direction of the applied field. The quadratic electro-optic coefficients for an isotropic crystal are given by

$$\begin{pmatrix} s_{11} & s_{12} & s_{12} & 0 & 0 & 0 \\ s_{12} & s_{11} & s_{12} & 0 & 0 & 0 \\ s_{12} & s_{12} & s_{11} & 0 & 0 & 0 \\ 0 & 0 & 0 & 1/2(s_{11} - s_{12}) & 0 & 0 \\ 0 & 0 & 0 & 0 & 1/2(s_{11} - s_{12}) & 0 \\ 0 & 0 & 0 & 0 & 0 & 1/2(s_{11} - s_{12}) \end{pmatrix} \quad \text{Eqn. (3.30)}$$

The index of ellipsoid for such an isotropic medium on the application of E reduces to

$$x^2 \left(\frac{1}{n^2} + s_{12}E^2 \right) + y^2 \left(\frac{1}{n^2} + s_{12}E^2 \right) + z^2 \left(\frac{1}{n^2} + s_{11}E^2 \right) = 1 \quad \text{Eqn. (3.31)}$$

Where s_{12} and s_{11} are the quadratic electro-optic coefficients and E is the magnitude of the applied electric field.

$$n_0 = n - \frac{1}{2}n^3s_{12}E^2 \quad \text{Eqn. (3.32)}$$

$$n_e = n - \frac{1}{2}n^3s_{11}E^2 \quad \text{Eqn. (3.33)}$$

The birefringence $n_e - n_0$ is given by

$$n_e - n_0 = n - \frac{1}{2}n^3(s_{12} - s_{11})E^2 \quad \text{Eqn. (3.34)}$$

By using the relationship $s_{44} = \frac{1}{2}(s_{12} - s_{11})$ can be written as

$$\Delta n = -n^3s_{44}E^2 \quad \text{Eqn. (3.35)}$$

The above equation is often written in terms of the Kerr coefficient (K) in m/V^2 as

$$\Delta n = K\lambda E^2 \quad \text{Eqn. (3.36)}$$

Where $s_{44} = -\frac{K\lambda}{n^3}$

This equation represents the relation between change in refractive index and the Kerr coefficient (K).

Chapter 4

NONCONJUGATED CONDUCTIVE POLYMERS

Organic polymers and inorganic materials have a wide range of applications in the field of photonics. Among organic materials, conjugated polymers having one-dimensional delocalization of electrons become electrically conductive upon doping. It was reported back in 1988 by M Thakur that conducting polymers are not limited to conjugated systems alone. It was reported that with an appropriate substituent a backbone having an isolated double-bond structure may become conducting. Thus new set of polymers came into existence called as nonconjugated conducting polymer. The first reported NCPs by Thakur and co-workers were: cis-1,4-polyisoprene, trans-1,4-polyisoprene and poly(dimethyl butadiene) [1]. Subsequently, poly(β -pinene) [37], polyalloocimene, polynorbornene and styrene-butadiene-rubber (SBR) [2], were shown by Thakur's group to belong to the class of nonconjugated conductive polymers. It was seen that the conductivity of the polymers increased many orders of magnitude with doping of iodine.

This chapter illustrates literature review on various nonconjugated conductive polymers that have been explored in this research work. These nonconjugated polymers include poly (β -pinene) (PBP), cis-1,4-polyisoprene (CPI), trans-1,4-polyisoprene (TPI) and a copolymer styrene-butadiene-rubber (SBR). Earlier study includes exploring the conductivity of non-conjugated polymers upon doping with iodine, SnCl_4 and SbCl_5 . The conductivity of nonconjugated polymer is based on number fraction of double bonds, which is the ratio of double bonds to the total number of bonds along the polymer chain. Upon doping, there is formation of radical cation and charge transfer from double bond to dopant which is primarily responsible for the non-conjugated polymers to become conductive. Conductivity increases rapidly with the

increase in the number fraction of double bonds. Conjugated polymers have double bonds alternating with single bonds; as a result their number fraction of double bonds is $\frac{1}{2}$, while non-conjugated conductive polymers have double bond number fractions less than $\frac{1}{2}$ [1, 2, 3]. Mentioned below are few specific non conjugated polymers on which the research has been carried out in this work.

4.1 Poly (β -pinene) (PBP)

PBP has been reported as novel nonconjugated polymer. It has ring type structure, in which double bond repeats after every sixth carbon; therefore it has $\frac{1}{6}$ number fraction of double bonds and its conductivity increases rapidly upon doping with iodine. The molecular structure poly (β -pinene) is shown in the figure below.

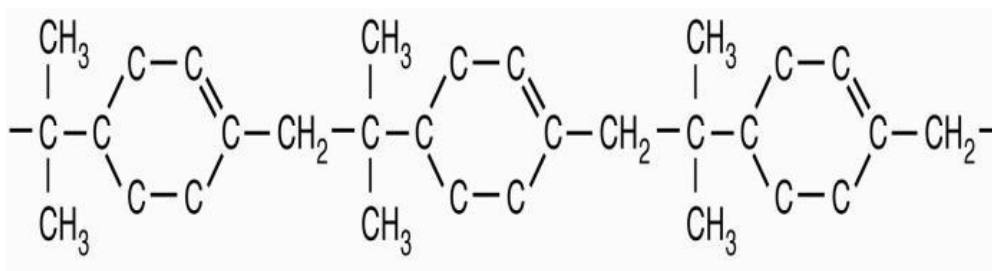


Figure 4.1 Molecular structure of Poly(β -pinene)

Conductivity of PBP has been measured before and after doping with iodine, it increased by many orders of magnitude upon doping with iodine (0.008 S/cm). This is due to formation of radical cation and charge transfer from double bond to dopant. PBP shows large nonlinear properties and have large Kerr coefficient, $1.6 \times 10^{-10} \text{ m/V}^2$ at 1550 nm [40, 41].

4.2 Polyisoprene

Polyisoprene shows two conformations: *cis*-1,4-polyisoprene and *trans*-1,4-polyisoprene. Both have the same molecular formula but the carbon atoms are oriented differently in structure. In both, every fourth carbon has double bond; number fraction of double bond is $\frac{1}{4}$ and their conductivity also increases by many orders of magnitude after doping with iodine [1, 3]. They have maximum conductivity of ~ 0.1 S/cm. Polyisoprene (natural rubber) is used non conjugated conductive polymers have a wide range of applications in antistatic, various sensors and optoelectronics.

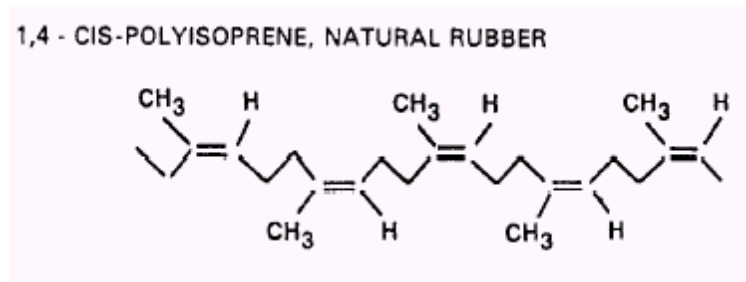


Figure 4.2 Undoped Polyisoprene

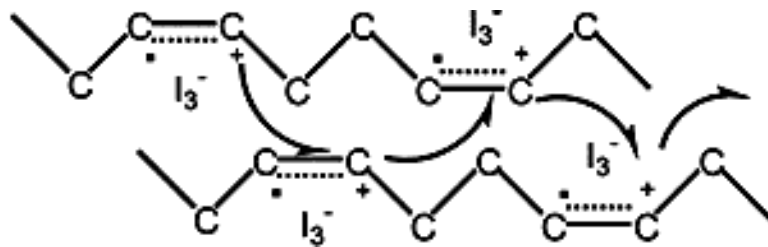


Figure 4.3 Schematic of the intersite hopping transport in a doped nonconjugated conductive polymer (polyisoprene)

Figure below shows the electrical conductivities of *cis*-polyisoprene (natural rubber), *trans*-polyisoprene, and poly (dimethylbutadiene) for different molar concentrations (y) of iodine.

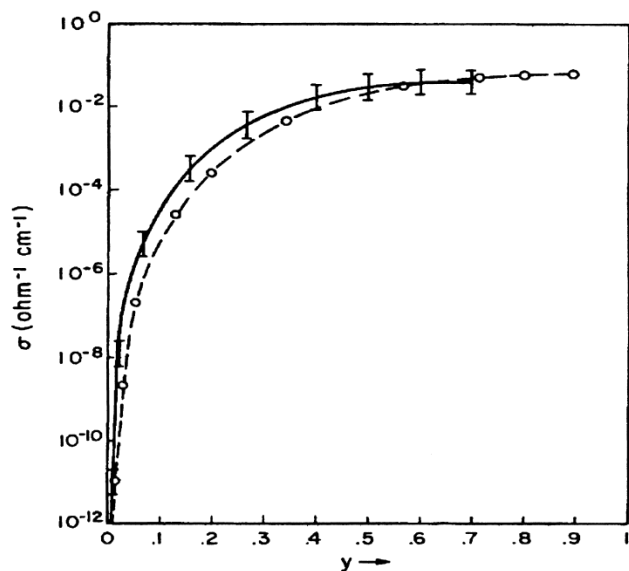


Figure 4.4 The electrical conductivities for cis- and trans- polyisoprene lie on the solid curve and the data for poly (dimethylbutadiene) lie on the dashed curve. From Reference 2 (Macromolecules 1988)

4.2.1 Cis-1,4-polyisoprene (CPI)

Cis-1,4-polyisoprene is also known as natural rubber. It is a predominantly amorphous polymer and gives smooth film when deposited on glass slide from a solution. The electrical conductivity of cis-1,4-polyisoprene increases 100 billion times upon doping with iodine. The molecular structure of cis-1,4-polyisoprene is shown in Figure.4.5.

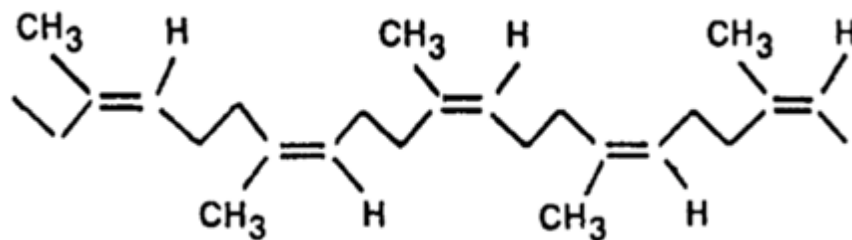


Figure 4.5 Molecular structure of Cis-1,4-polyisoprene

Absorption spectra of cis-polyisoprene before and after iodine-doping are shown in

Figure 4.6. Kerr coefficient for cis-polyisoprene has already been reported, which is 1.6×10^{-10} m/V^2 and higher than Poly (β -pinene) [1]

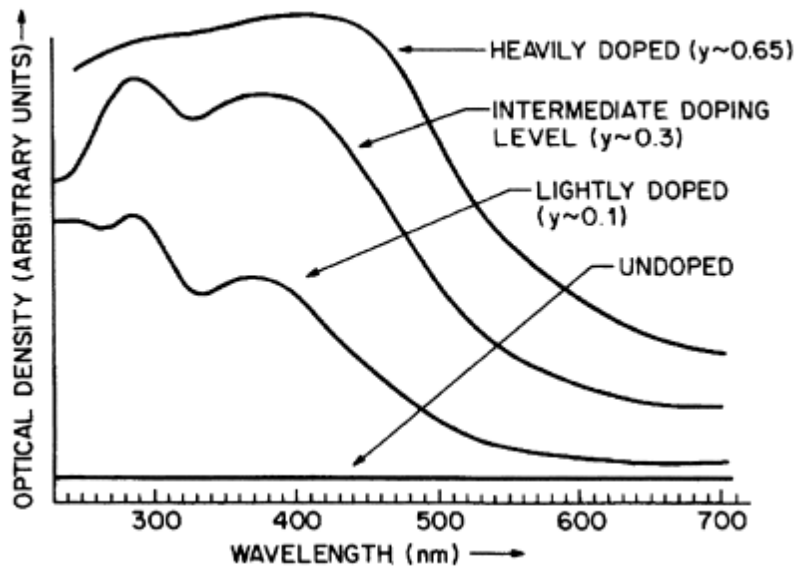


Figure 4.6 Absorption Spectra of CPI at different doping level with iodine (ref.1)

4.2.2 Trans-1,4-polyisoprene (TPI)

Trans-1,4-polyisoprene is a polycrystalline material with a planar zig-zag molecular structure. Recently it is known for its conductivity upon doping with iodine. The molecular structure of trans-1,4-polyisoprene is shown in the Figure below.

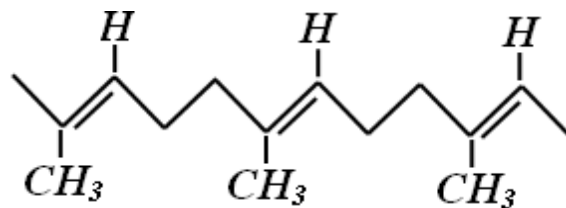


Figure 4.7 Molecular structure of Trans-1, 4- polyisoprene [42]

Characterization had done of TPI by study of its thin film with optical absorption, FTIR, X-ray diffraction. Kerr coefficient for trans-1,4-polyisoprene has already been reported to be 1.6×10^{-10} m/V², which is higher than Poly(β -pinene) [1, 2, 42].

4.3 Styrene-butadiene-rubber (SBR)

Styrene-Butadiene-Rubber (SBR) is a synthetic rubber copolymer consisting of styrene and butadiene. It generally finds its application in car tires due to its ability to have good abrasion resistance [43]. Styrene-butadiene-rubber is nonconductive in its normal state. It becomes conductive upon doping with doping agents like iodine, SnCl₄ and SbCl₅. Styrene-butadiene-rubber was doped with iodine and it was noticed that the conductivity of the styrene-butadiene-rubber film reaches a value of about 0.01 S/cm and then the value remains a constant as the film is saturated with the iodine. The fact that the film darkens upon doping is attributed to the breaking up of the double bonds. The molecular structure of styrene-butadiene-rubber is shown in the figure below.

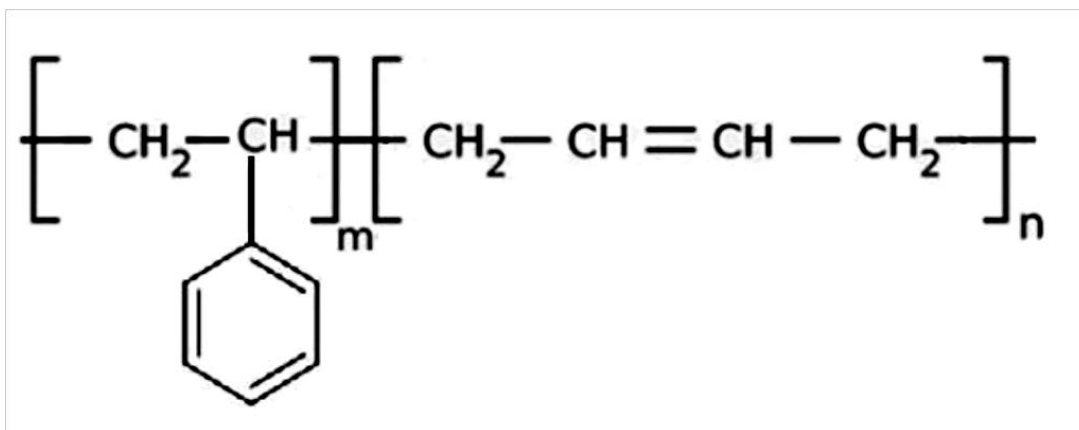


Figure 4.8 Molecular structure of styrene-butadiene-rubber

This research work has been undertaken to study structures of iodine doped Nonconjugated conductive polymers, Cis-polyisoprene and Poly (β -pinene), and their large nonlinear optical properties.

Chapter 5

PHOTOVOLTAIC CELLS INVOLVING NONCONJUGATED CONDUCTIVE POLYMER IODINE-DOPED POLY(β -PINENE)

5.1 Introduction

Energy drives the universe. We need energy to do anything and everything in our daily life. We are totally dependent on the supply of energy. The increase in world population is increasing the need for energy. It is estimated that the world population will be nearly doubled by the end of the twenty first century which will increase energy demand by nearly two fold. The world population statistics from 1950 and the projected population statistics till 2050 are shown below.

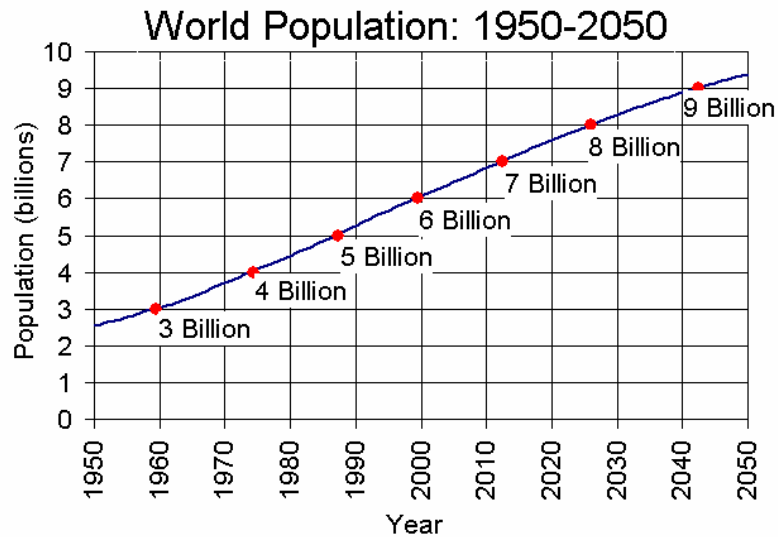


Figure 5.1 World Population statistics [44]

The population is projected to increase to 9 billion by 2042, which is nearly 50% increase from the year 1999. This would thereby cause an increase in the world energy consumption. The

world energy consumption from 1980 and the projected energy consumption till 2030 is shown below [45, 46].

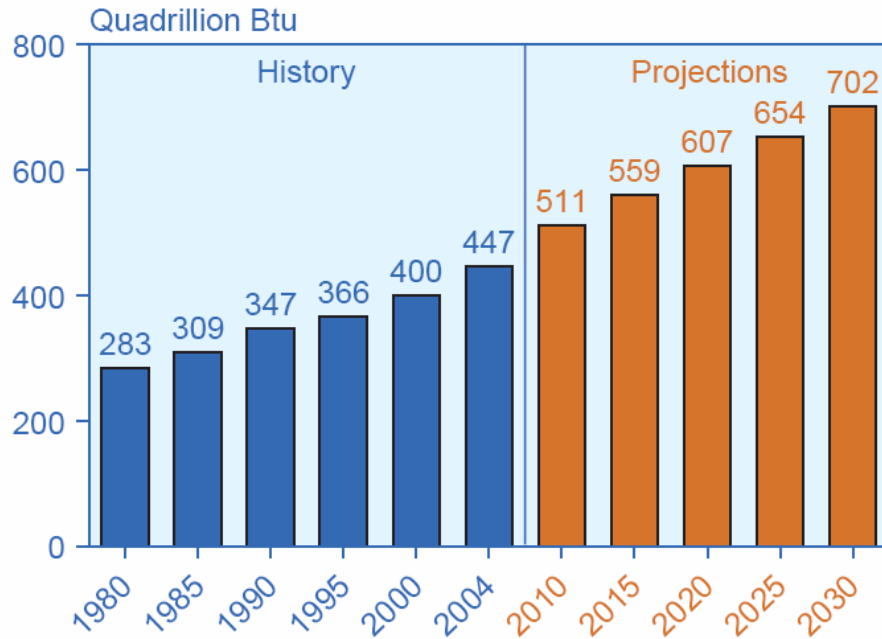


Figure 5.2 World Energy Consumption from 1980-2030

It is estimated that in 2030 the world energy need is projected to go nearly by 40%-50% of the present need. At present around 86.5% of the world energy needs are supplied through burning fossil fuels [47]. This has resulted into advent of the need for exploring energy from the renewable resources. And photovoltaic is one such way to generate energy from a renewable source.

Sun is one of the most abundant sources of energy that we know till now. There are two types of energy source namely renewable and nonrenewable. The renewable consist of solar energy, wind energy etc. where else nonrenewable consist of fossil fuels, oil, and petroleum etc. However today, the need of exploring new ways to obtain energy from these renewable sources has gained attention of many researchers. This need is mainly due to the excessive utilization of nonrenewable resources in this modern world.

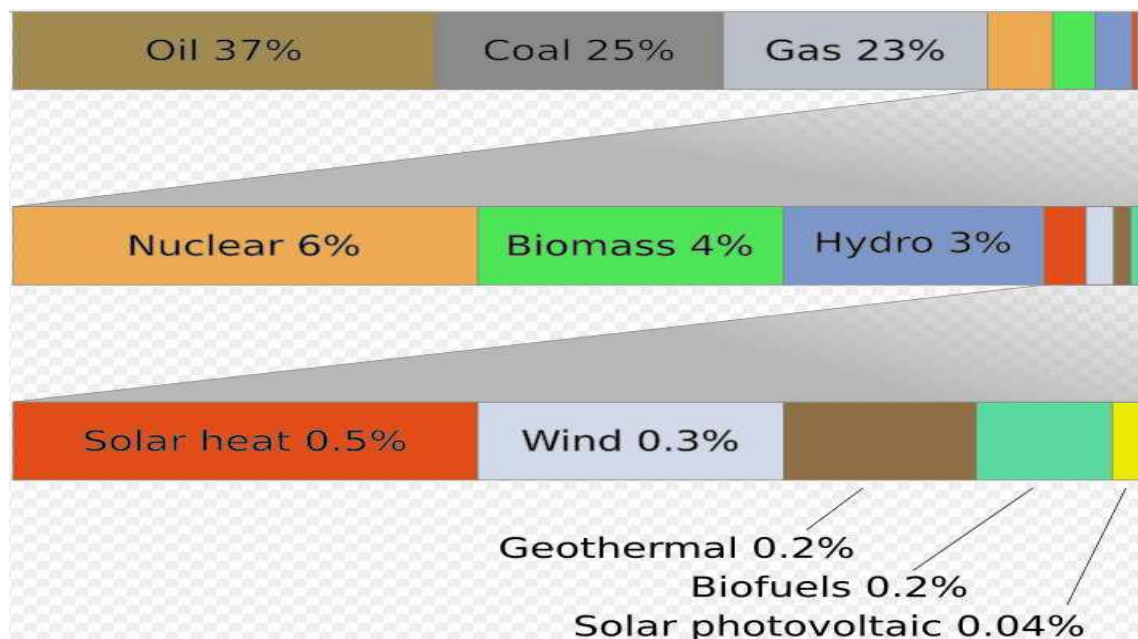


Figure 5.3 World energy consumption by energy source [48, 49]

Organic polymers have attracted a great deal of interest in the area of photovoltaic. Photovoltaic are a field in which light energy is used to produce electric current by movement of free electrons. These materials show promising results and can serve as lower cost alternatives to inorganic photovoltaic materials. The first two-layer organic photovoltaic system appears to have been reported in 1958. Poly(p-phenylene vinylene) (PPV) has been widely studied in the area of organic photovoltaic devices. Exploration in the field of photovoltaic devices based on polythiophene has also been reported. The incident light is responsible to produce electron from such organic materials resulting into generation of electric current. Earlier photo-induced electron-transfer between conjugated polymer and C₆₀ leading to photovoltaic effects have been investigated in detail.

5.2 Experiment

Glass substrates with a conductive indium-tin-oxide (ITO) coating on one of the surfaces were used to fabricate the electrodes of the photo-voltaic cells. The coating was identified using a high impedance electrometer (Keithley 617 Programmable electrometer). A thin coating of carbon was deposited using a candle on the ITO layer of one of the glass substrates and was used as one of the electrodes. A film of poly(β -pinene) (area $\sim 5\text{cm}^2$) was deposited on the carbon layer from a toluene solution. The poly(β -pinene) film was doped with iodine to a high level (~ 0.8 molar) following standard procedure [50]. The molecular structure of poly(β -pinene) before and after doping is shown in Fig.5.4. The optical absorption spectra of poly(β -pinene) for different doping levels of iodine are shown in Fig.5.5. To prepare the second electrode, nano-crystalline titanium dioxide (from Sigma-Aldrich) was ground. Drops of dilute acetic acid and triton X-100 were added to the titanium dioxide to form a viscous liquid. A thin layer of this mixture was spread on the ITO layer of the second glass substrate. This titanium dioxide-coated substrate was then heated for 15-20 minutes and subsequently cooled slowly to prepare the second electrode. The two glass substrates with the aforementioned layers were brought in contact with each other to form the photovoltaic cell. To maintain good contact, alligator clips were used. A solution of 1-methyl-3-propylimidazolium iodide in ethylene glycol was prepared (1:4). A few drops of this solution were introduced into the cell from the side. This cell was then left idle for about 4-5 hours so that the 1-methyl-3-propylimidazolium iodide could spread uniformly throughout the plates and also to make the cell free of residual charges.

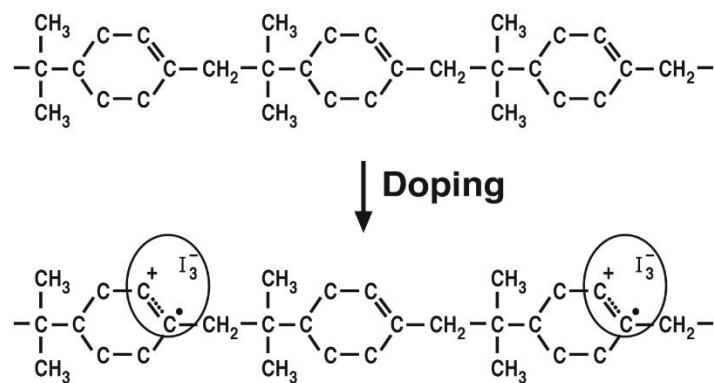


Figure 5.4 Molecular structure of poly(β -pinene) before and after iodine-doping

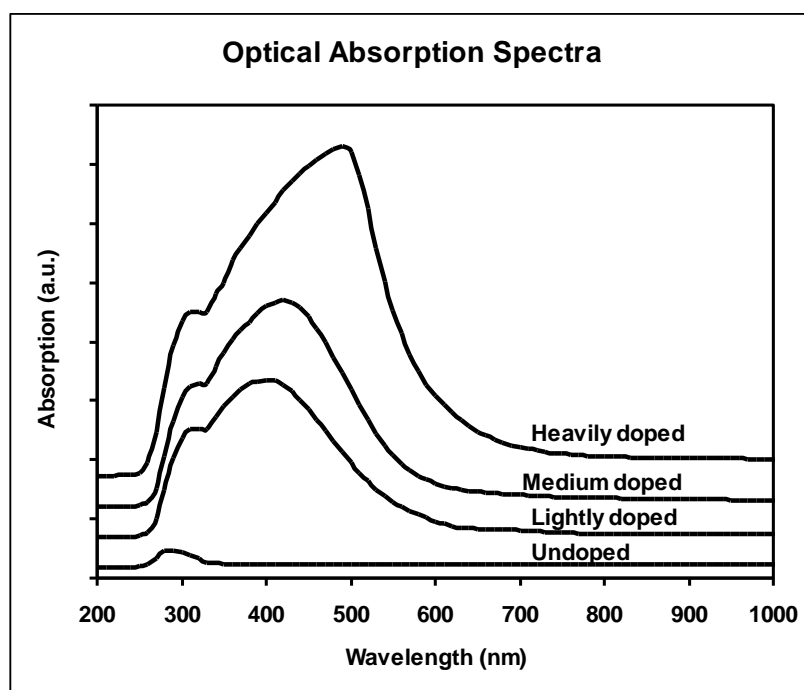


Figure 5.5 Optical absorption spectra of poly(β -pinene) for different doping levels of iodine. The heavily doped samples as used here correspond to iodine molar concentration of about 0.8

A light source with a broad emission spectrum was used to measure the photo-voltaic effect. The light source was placed in such a way that the light was incident on the doped poly(β -pinene) film through the titanium-dioxide-coated transparent electrode. Photo-voltages and photocurrents as a function of light intensity were recorded. The open-circuit voltages and short-circuit currents for different light intensities were measured using a high impedance electrometer (Keithley 617 programmable electrometer). The intensity of light was measured using a power meter (Newport model 1916-R). The experimental setup is shown in Figure 5.6.

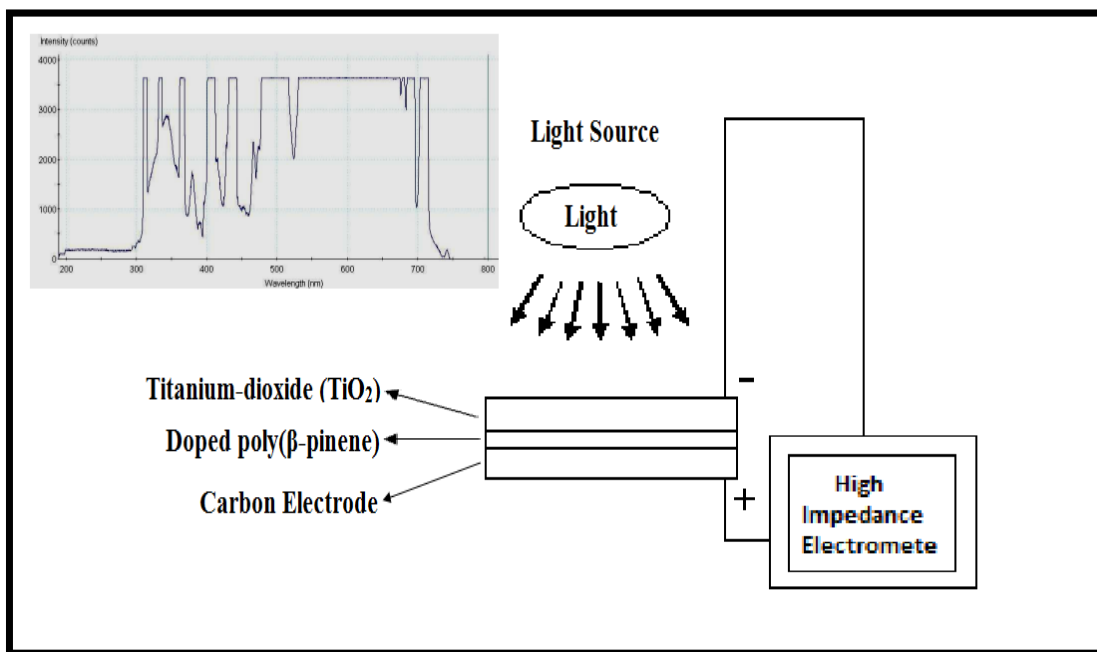


Figure 5.6 Experimental set-up for photo-voltaic measurements. The inset shows the emission spectrum of the light source used in the experiment

5.3 Results and Discussion:

The photocurrent vs. light intensity and photo-voltage vs. light intensity data have been plotted and are as shown in figures 5.7 and 5.8 respectively. The current and voltage increased as the light intensity was increased. A maximum photocurrent of about 300 μ A and a maximum photo-voltage of about 0.6 V were produced for a light intensity of 5mW/cm².

The mechanism of the photovoltaic effect is as follows. As the incident light is absorbed by the doped polymer electron hole pairs are produced. The electrons are transferred to the TiO₂ electrode and transported through the leads to the carbon electrode. Then these electrons interact with the I⁻/I₃⁻ redox couple (electrolyte: 1-methyl-3-propylimidazolium iodide) to return the polymer-molecular system to the original state and thus completing the cycle. This process is responsible for the photovoltaic effect. The photovoltages and currents are significantly higher compared to previously reported photovoltaic cells of undoped nonconjugated conductive polymer.

In future research, the thickness carbon layer and poly(β -pinene) should be considered. While doing literature review it was noted that the titanium oxide layer should be thinner to produce better results. Upon doing this, the cells were frequently shorting and more research is required to solve the problem. Further research is in progress to make multiple photovoltaic cells and observe the photovoltaic effects in different types of connections.

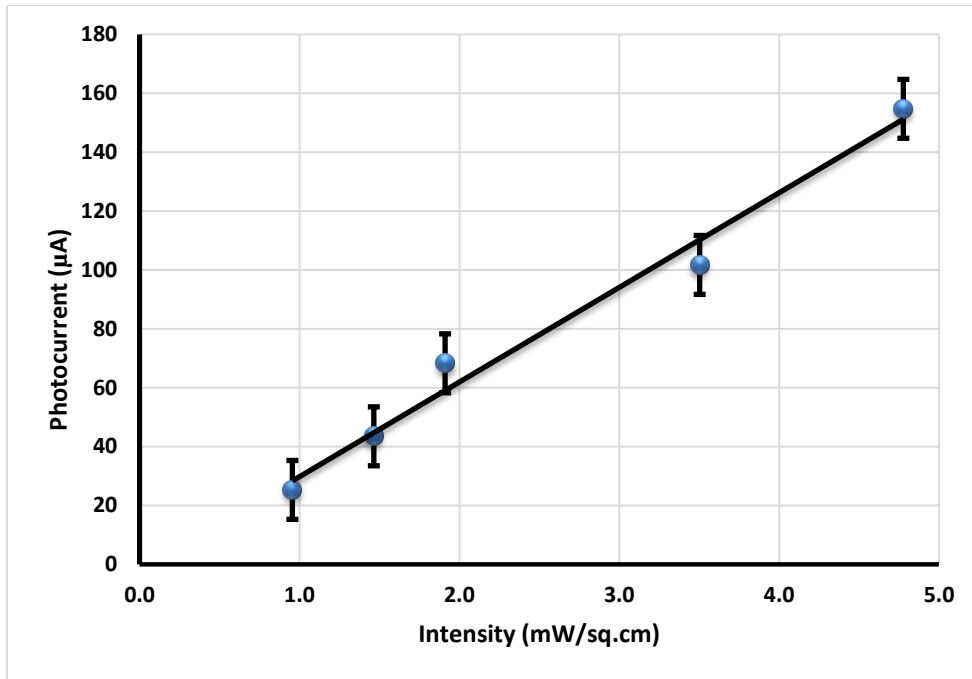


Figure 5.7 Measured photocurrent for different light intensities. The area of the device was $\sim 5 \text{ cm}^2$

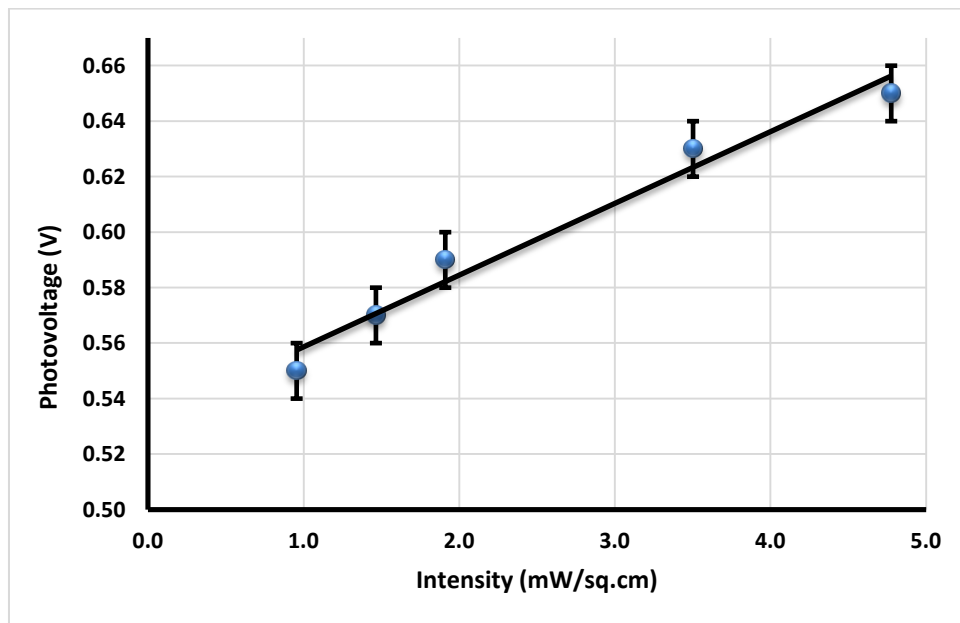


Figure 5.8 Measured photo-voltages for different light intensities. For dark condition the measured voltage was about 50 mV

5.4 Conclusion

Photovoltaic cells involving the nonconjugated conductive polymer, iodine-doped poly(β -pinene) between TiO_2 and carbon electrodes have been fabricated. The maximum photocurrents and photo-voltages as observed for such cells are $300 \mu\text{A}$ and 0.6 V respectively for a light intensity of about 6 mW/cm^2 . The operation mechanism of these cells (Gratzel type) is as follows: i) absorption of incident light generates electrons and holes in the doped nonconjugated conductive polymer, ii) these electrons are transferred to TiO_2 and they subsequently complete the circuit. These electrons return through the carbon electrode to recombine with holes leading to the original state. Thus photocurrent / photovoltaic effect is produced. The cells reported here may provide a less expensive alternative to other reported photovoltaic cells. This photovoltaic cell finds itself into various fields of applications providing cheaper cost in the areas of solar cells, photo-detectors, photo sensors etc.

Chapter 6

PHOTOVOLTAIC CELLS INVOLVING NONCONJUGATED CONDUCTIVE POLYMER IODINE-DOPED CIS-1,4-POLY(ISOPRENE)

6.1 Introduction

In this chapter we discuss about the fabrication of photovoltaic cells involving nonconjugated conductive polymer, iodine-doped **cis-1,4-polyisoprene**. Cis-1,4-polyisoprene is one such nonconjugated polymer which becomes electrically conductive upon doping with an electron acceptor [1]. Many other polymers with nonconjugated backbone like 1, 4 polybutadiene, polyalloocimine and poly(β -pinene) were studied for their optical and electrical properties. The characterization of CPI of its thin film with optical absorption, FTIR, X-ray diffraction and other spectroscopic methods has been done earlier. Kerr coefficient for cis-1,4-polyisoprene has been already reported to be $1.6 \times 10^{-10} \text{ m/V}^2$, which is higher than Poly(β -pinene) reflects that they are in nanometallic range. Photocurrents and photovoltages have been observed and have been plotted along light intensity.

6.2 Experiment

Glass substrates with a conductive indium-tin-oxide (ITO) coating on one of the surfaces were used to fabricate the electrodes of the photo-voltaic cells. The coating was identified using a high impedance electrometer (Keithley 617 Programmable electrometer). A thin coating of carbon was deposited using a candle on the ITO layer of one of the glass substrates and was used as one of the electrodes. A film of cis-1,4-poly(isoprene) (area $\sim 5 \text{ cm}^2$) was deposited on the carbon layer from a toluene solution. The cis-1,4-poly(isoprene) film was doped with iodine to a high level (~ 0.8 molar) following standard procedure. The molecular structure of cis-1,4-poly(isoprene) before and after doping are shown in Fig.6.1 and 6.2 respectively. The optical

absorption spectra of cis-1,4-poly(isoprene) for different doping levels of iodine are shown in Fig.6.3. To prepare the second electrode, nano-crystalline titanium dioxide (from Sigma-Aldrich) was ground. Drops of dilute acetic acid and triton X-100 were added to the titanium dioxide to form a viscous liquid. A thin layer of this mixture was spread on the ITO layer of the second glass substrate. This titanium dioxide-coated substrate was then heated for 15-20 minutes and subsequently cooled slowly to prepare the second electrode. The two glass substrates with the aforementioned layers were brought in contact with each other to form the photovoltaic cell. To maintain good contact, alligator clips were used. A solution of 1-methyl-3-propylimidazolium iodide in ethylene glycol was prepared (1:4). A few drops of this solution were introduced into the cell from the side. This cell was then left idle for about 4-5 hours so that the 1-methyl-3-propylimidazolium iodide could spread uniformly throughout the plates and also to make the cell free of residual charges.

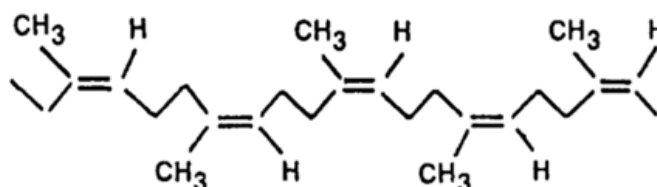


Figure 6.1: Molecular structure of Cis-polyisoprene

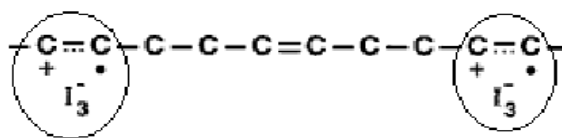


Figure 6.2 Molecular structure of cis-1,4-poly(isoprene) after iodine-doping

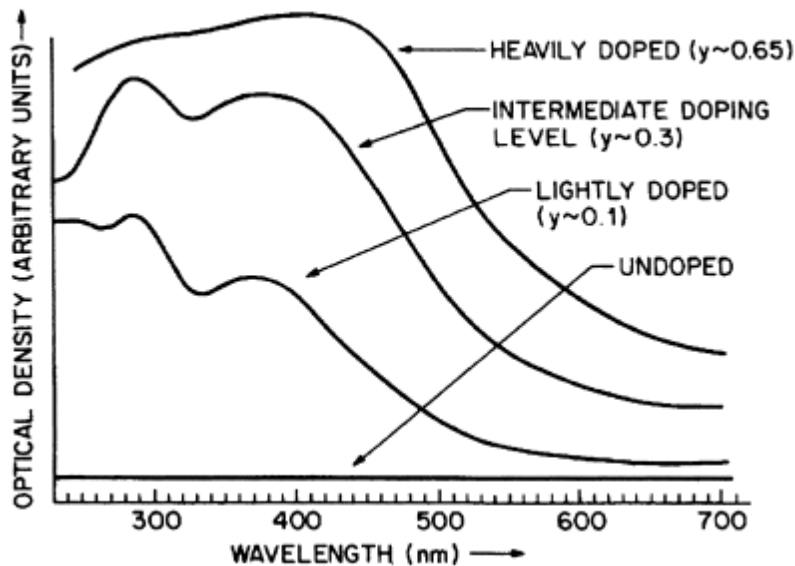


Figure 6.3 Optical absorption spectra of 1,4 cis-polyisoprene at different doping levels. y -molar concentration of iodine (From ref.1)

A light source with a broad emission spectrum was used to measure the photo-voltaic effect. The light source was placed in such a way that the light was incident on the doped cis-1,4-poly(isoprene) film through the titanium-dioxide-coated transparent electrode. Photo-voltages and photocurrents as a function of light intensity were recorded. The open-circuit voltages and short-circuit currents for different light intensities were measured using a high impedance electrometer (Keithley 617 programmable electrometer). The intensity of light was measured using a power meter (Newport model 1916-R). The experimental setup is shown in Figure 6.4.

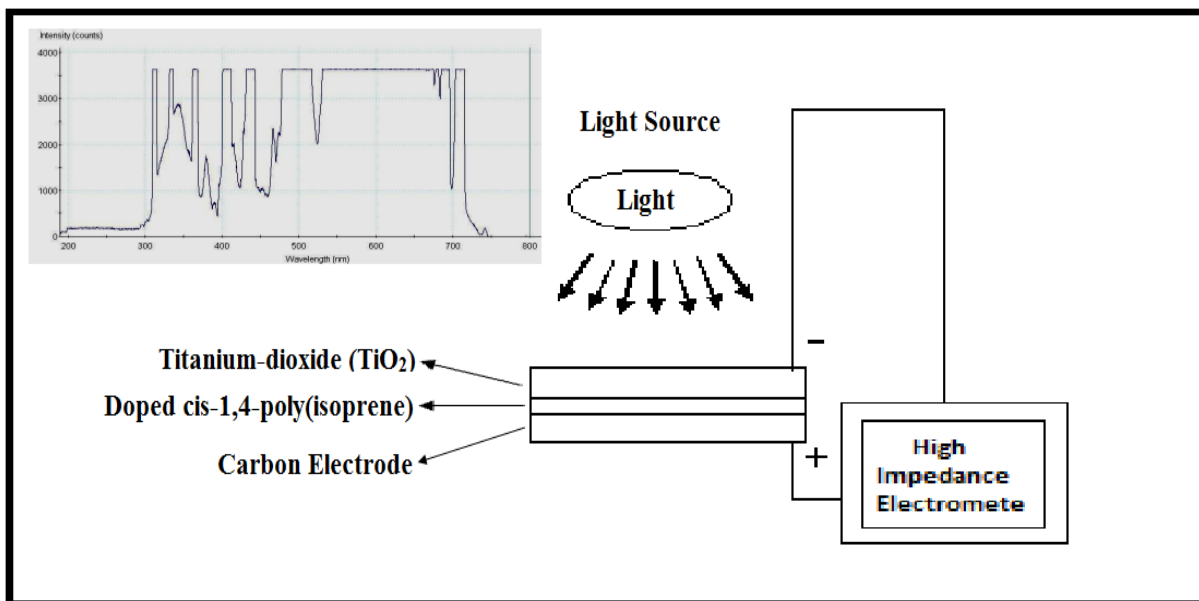


Figure 6.4 Experimental set-up for photo-voltaic measurements. The inset shows the emission spectrum of the light source used in the experiment

6.3 Results and Discussion

The photocurrent vs. light intensity and photo-voltage vs. light intensity data have been plotted and are as shown in figures 6.5 and 6.6 respectively. The current and voltage increased as the light intensity was increased. A maximum photocurrent of about 250 μ A and a maximum photo-voltage of about 0.75 V were produced for a light intensity of \sim 5mW/cm².

The mechanism of the photovoltaic effect is as follows (figure 6.7). As the incident light is absorbed by the doped polymer electron hole pairs are produced. The electrons are transferred to the TiO₂ electrode and transported through the leads to the carbon electrode and return to the molecular structure. These electrons combine with the holes completing the cycle. This process is responsible for the photovoltaic effect. The photovoltages and currents are

significantly higher compared to previously reported photovoltaic cells of undoped nonconjugated conductive polymer.

In future research, the thickness carbon layer and cis-1,4-poly(isoprene) should be considered. While doing literature review it was noted that the titanium oxide layer should be thinner to produce better results. Upon doing this, the cells were frequently shorting and more research is required to solve the problem. Further research is in progress to make multiple photovoltaic cells and observe the photovoltaic effects in different types of connections.

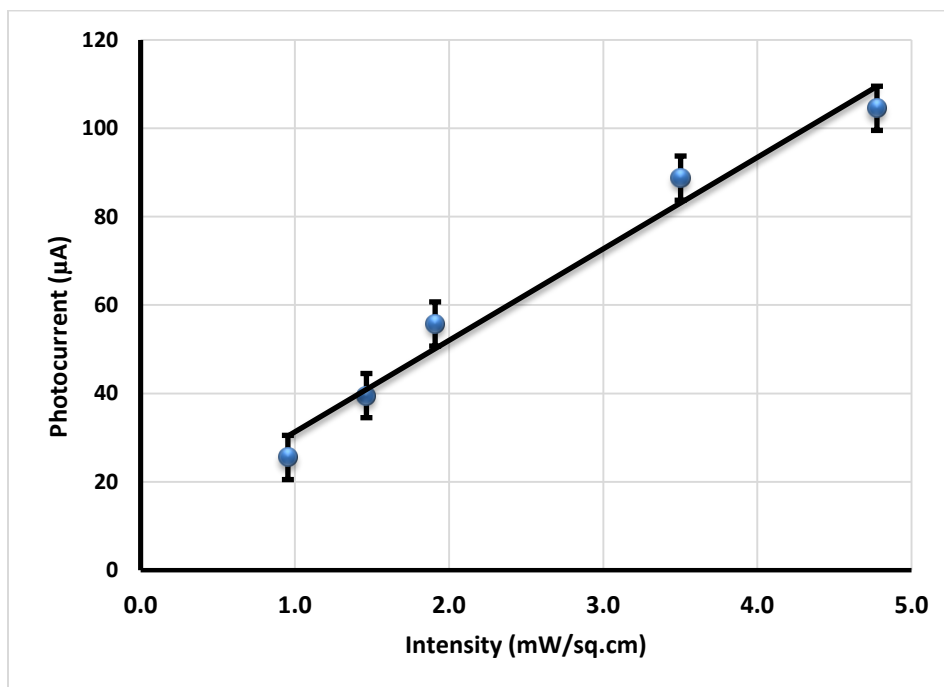


Figure 6.5 Measured photocurrent for different light intensities. The area of the device was $\sim 5 \text{ cm}^2$

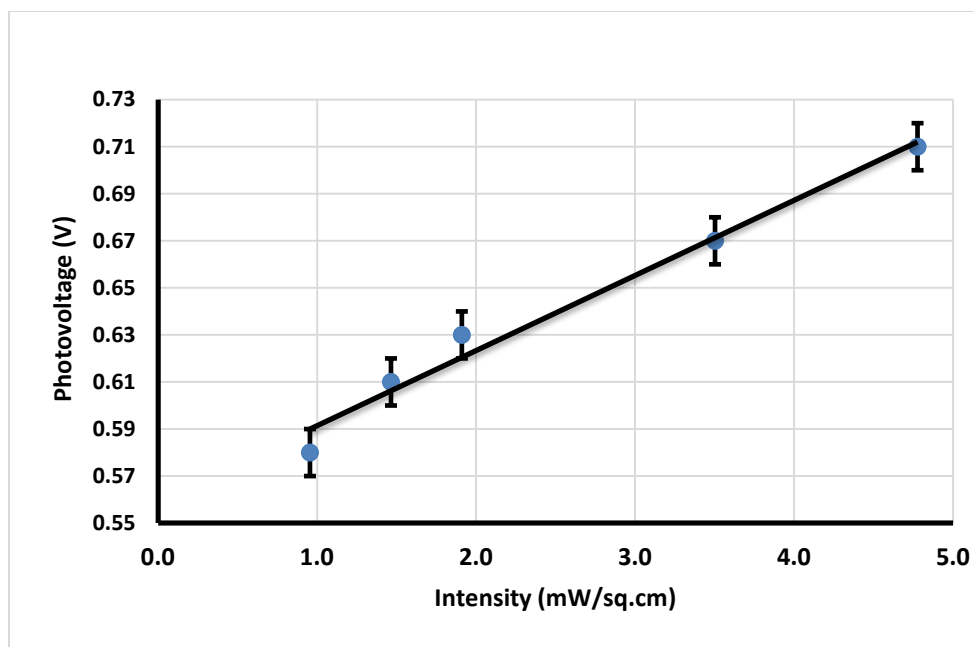


Figure 6.6 Measured photo-voltages for different light intensities. For dark condition the measured voltage was about 40 mV

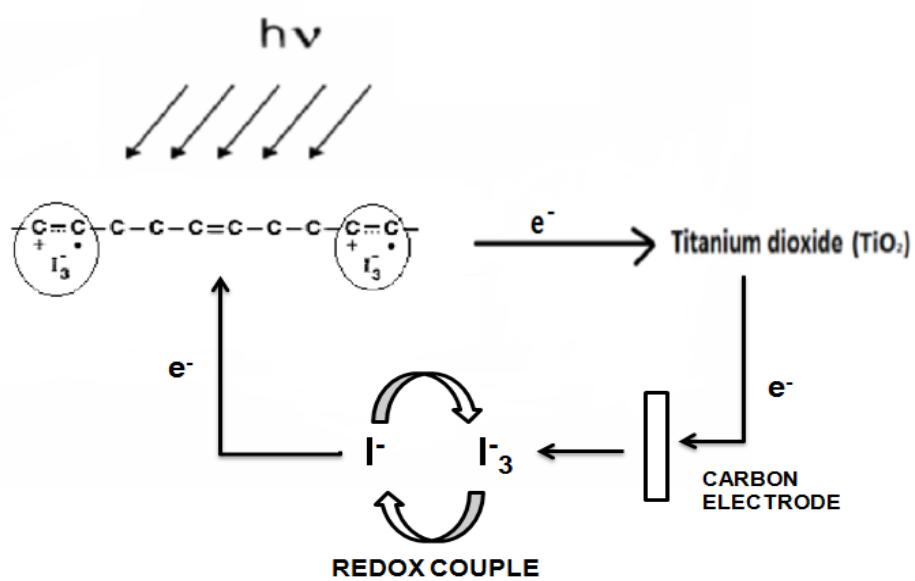


Figure 6.7 A schematic of the mechanism involved in the photovoltaic effect in these cells.

6.4 Conclusion

Photovoltaic cells involving the nonconjugated conductive polymer, iodine-doped cis-1,4-poly(isoprene) between TiO₂ and carbon electrodes have been fabricated. The maximum photocurrents and photo-voltages as observed for such cells are 0.25mA and 0.75 V respectively for a light intensity of about 6mW/cm². The operation mechanism of these cells (Gratzel type) is as follows: i) absorption of incident light generates electrons and holes in the doped nonconjugated conductive polymer, ii) these electrons are transferred to TiO₂ and they subsequently complete the circuit. These electrons return through the carbon electrode to recombine with holes leading to the original state. Thus photocurrent / photovoltaic effect is produced. The cells reported here may provide a less expensive alternative to other reported photovoltaic cells. This photovoltaic cell finds itself into various fields of applications providing cheaper cost in the areas of solar cells, photo-detectors, photo sensors etc.

CHAPTER 7

QUADRATIC ELECTRO-OPTIC MODULATION IN NONCONJUGATED CONDUCTIVE POLYMER 1,4-CIS-POLYISOPRENE

7.1 Introduction

Materials and structures of confined dimensions are important for fundamental studies and various novel technological applications. Nonlinear optical characteristics were known to substantially enhance for confined electronic systems [1-3, 9]. Among organic materials, conjugated polymers are known as quantum wires because of one-dimensional delocalization of electrons. Recently, nonconjugated conductive polymers have been shown to have quantum dot characteristics because of the confinement of charges within subnanometer domains. Such confinement has led to significantly larger third order optical nonlinearities for these systems compared to known materials and structures.

Quadratic electro-optic effect in nonconjugated conductive polymers including poly(β -pinene), styrene-butadiene-rubber, poly(ethylenepyrrrolediyl) derivative and polynorbornene have been recently reported [1-3,41,42,50]. Exceptionally large Kerr-coefficients (about 30 times that of conjugated polymers) have been observed in these systems.[35] In the present article, we discuss structural and nonlinear optical property; in particular, quadratic electro-optic effect in the nonconjugated conductive polymer, iodine-doped 1,4-cis-polyisoprene.

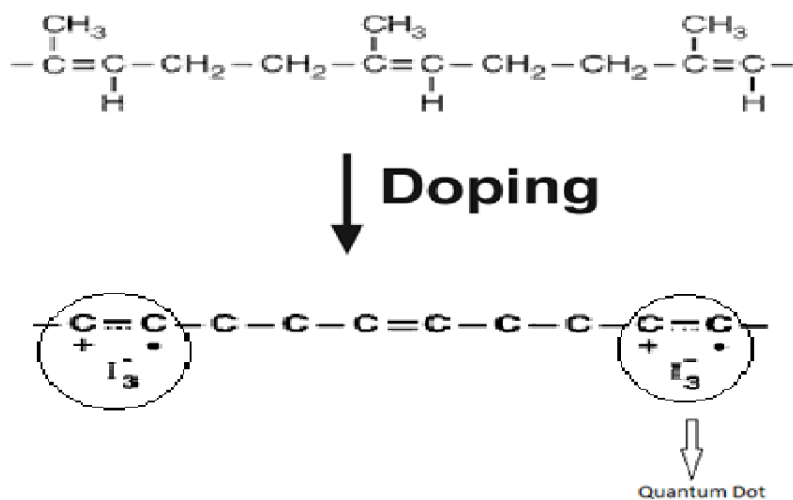


Figure 7.1 Transformation of double bond into cation radicals

7.2 Optical Absorption

As reported earlier, optical absorption measurements of cis-polyisoprene films were made at various doping levels of iodine in cis-polyisoprene.[1] Sample made on glass slide were used for optical absorption. It was recorded that the absorption of undoped cis-polyisoprene to be clearly transparent as shown in Figure 7.2, but at low doping it shows two peaks, one due to formation of cation radicals at $\sim 4.27\text{eV}$ and second due to charge transfer between double bond and dopants (electron acceptors) at $\sim 3.3\text{eV}$. As the dopant concentration is increased the overall absorption increases and the spectrum becomes broader. At high doping (iodine molar concentration ~ 0.7), the film becomes dark and absorbs throughout the visible region. The experiments performed here involved films with doping levels in the intermediate to high range (molar concentration 0.3-0.8). The wavelength used (633nm) was away from the absorption maximum (400-450nm).

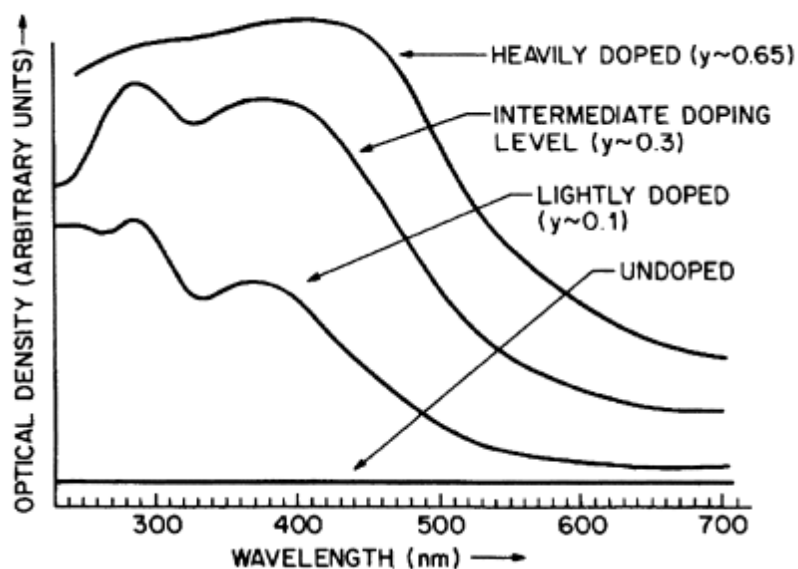


Figure 7.2 Optical absorption spectra of 1,4 cis-polyisoprene at different doping levels. y -molar concentration of iodine (From ref.1)

7.3 Sample preparation for Electro-optic experiment

Cis-1,4-Polyisoprene or natural rubber samples were obtained in the form of latex from Firestone Inc. Diluted latex was deposited as a film on a glass slide and was left undisturbed for 24 hours for the water to be evaporated. These films were then doped with iodine by evaporation in a closed container. Upon doping the films change color from colorless to black depending on the amount of dopant, iodine that has interacted with the cis-1,4-polyisoprene film. Thicker films and a high level of doping were used for the present measurement. Copper electrodes with a gap of about 200 μ m were used to apply the electric field for the electro-optic measurements.

7.4 Experimental setup

The doped film was studied for nonlinear optical properties with electric field applied across the copper electrodes. A helium-neon laser with wavelength at 633nm was used for the experiment. The method of measurement included field-induced birefringence in the cross-polarized geometry. A schematic of the electro-optics setup is shown in figure 7.3. the laser beam with polarization at 45 with respect to the applied electric field was passed through the sample. After passing through the analyzer which was oriented orthogonal to the polarizer, the beam was detected with a photodiode and recorded on the oscilloscope. An AC voltage at 4KHz was applied across the sample with the help of two copper electrodes to create an electric field. The resulting modulation due to quadratic electro-optic effect is recorded in a lock-in-amplifier (with $2f$ synchronization). The signal increased quadratically with the applied voltage.

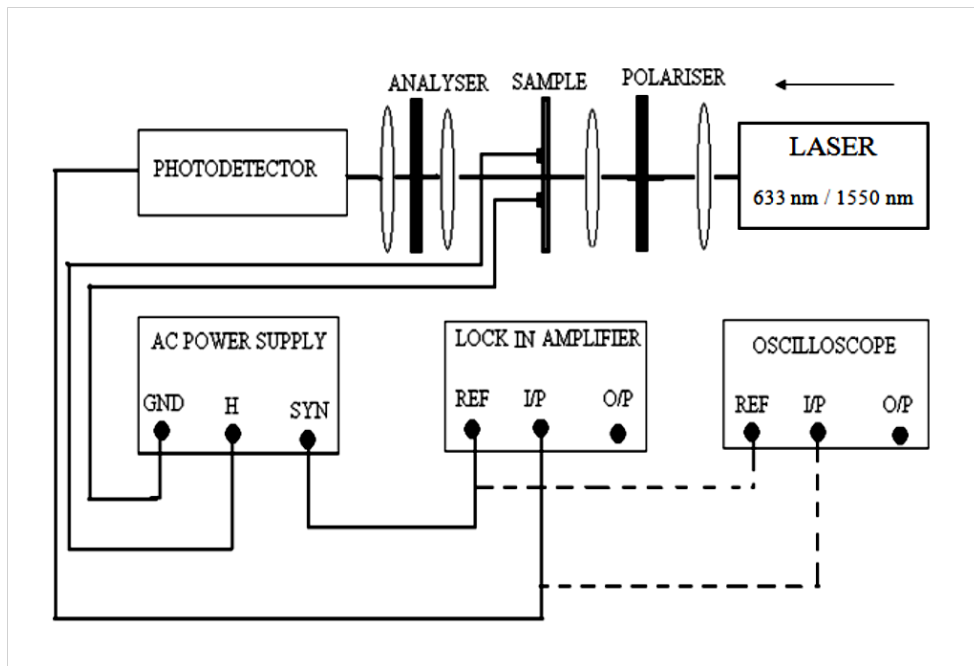


Figure 7.3: Experimental setup for electro-optics

7.4.1 Results

A quadratic electro-optic effect was observed in presence of an applied ac field. Modulation depth of 5% was observed for the very first time for an applied field of $\sim 1 \text{ V}/\mu\text{m}$ for a $50\mu\text{m}$ thick film, which is much higher than the modulation depths reported for such third order optical polymers. The modulation depth had a quadratic dependence on the applied ac field.

7.5 Experimental Setup for Guided Wave

Similar setup is created to measure the electro-optic effect in guided wave. The sample used here is an optical fiber. A part of core layer of the fiber is removed and then on the cladding part cis-polyisoprene solution (which contains toluene) is deposited. After 10min this sample is doped in iodine. The sample is kept in a dish in which iodine placed equally beside it. On doping for 7 hours the cladding parts color changes from colorless to black depending on the amount of iodine that has interacted with the cis-1, 4-polyisoprene solution. Then this fiber is placed on a glass slide with two copper electrodes in parallel to the fiber in such a way that the gap between the electrodes is covered with the fiber. Figure 7.4 shows the schematic view of the setup with the red part indicating as the doped fiber.

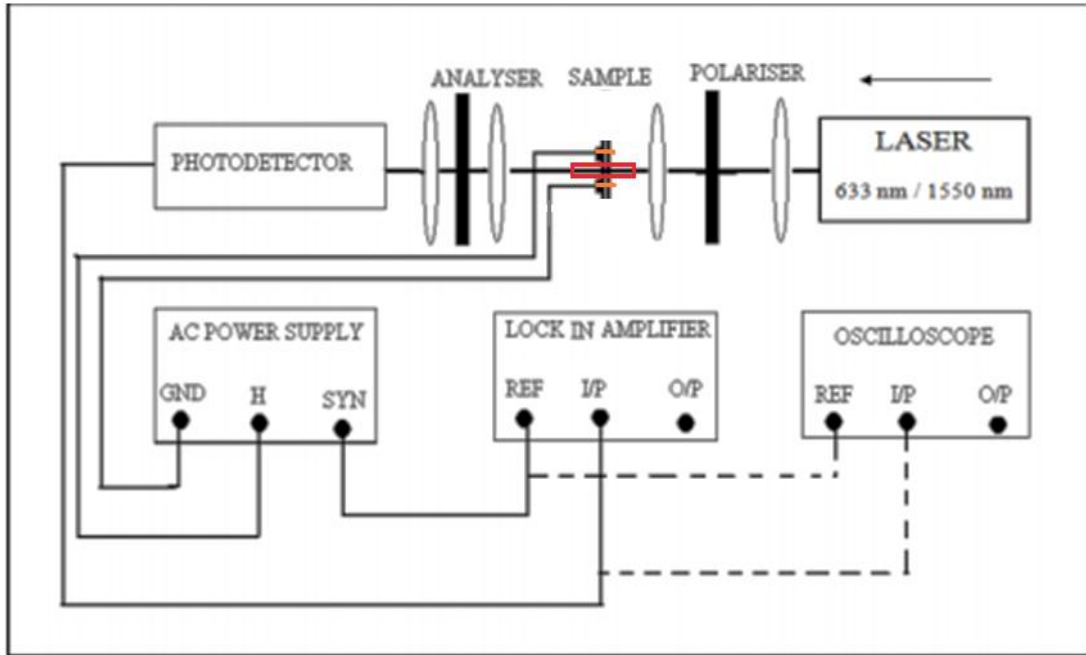


Figure 7.4: Experimental setup for Guided wave Electro-optics

7.5.1 Results

For the first time quadratic electro-optic modulation has been observed in a waveguide when ac field is applied. The throughput of the waveguide was 5% involving iodine doped nonconjugated conductive polymer covering an optical fiber of about 7 mm in length. The modulation depth observed for this waveguide was $\sim 1\%$ for an applied field of $0.3 \text{ V}/\mu\text{m}$. Figure 7.5 shows the modulation depth as a function of the applied electric field. Since optical coupling to the polymer film was significantly less than desirable the modulation depth was less. A modified design is needed to achieve higher modulation depth.

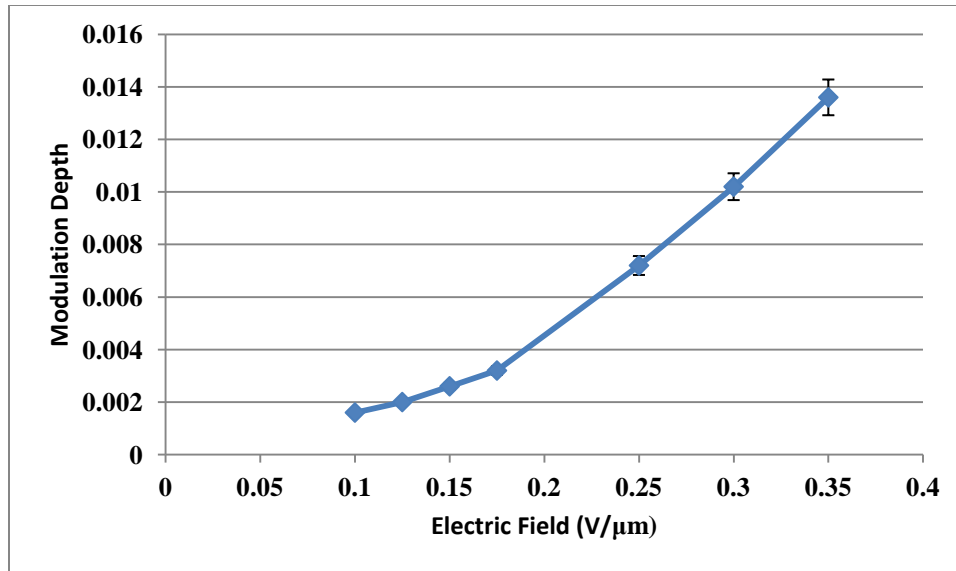


Figure 7.5 Quadratic modulation depth due to the applied Electric field.

7.6 Conclusion

There are two forms of natural rubber, one is cis-polyisoprene and other is trans-polyisoprene. Both of them show exceptionally large nonlinearities and quadratic effect. Cis-polyisoprene has third order susceptibility and Kerr coefficient of 3.4×10^{-8} esu (Estd.) and $1.6 \times 10^{-10} \text{m/V}^2$ respectively. Quadratic electro-optic effect of iodine doped nonconjugated conductive polymer cis-polyisoprene has been observed. Exceptionally large modulation depth of ~ 5% has been observed for the first time using thick (~ 50μm) film. Quadratic electro-optic effect for the guided wave of cis-polyisoprene has been reported for the first time in the field of photonics. The large Kerr Coefficient is observed due to charge transfer involving double bond of nonconjugated polymer and the sub-nanometer size nanometallic domains (encircled Region in (Figure 7.1) formed upon doping. These structures particularly represent novel metallic-like quantum dots of sub nanometer dimension for which enhanced optical nonlinearity can be expected. The electrical conductivity of these systems is comparable to that of metallic quantum dots / nanoparticles [51].

Chapter 8

SUMMARY

In summary, photovoltaic effect and quadratic electro-optic modulation in nonconjugated conductive polymers, poly(β -pinene) and cis-1,4-polyisoprene, have been studied. Photovoltaic cells has been fabricated using iodine-doped nonconjugated conductive polymers, poly(β -pinene) and cis-polyisoprene. Quadratic electro-optic modulation has been measured in the doped film of cis-polyisoprene at 633nm wavelength. Guided wave electro-optic effect has been reported for the first time using iodine doped cis-polyisoprene at 633nm.

For both of the photovoltaic cells, current and voltage increased as the light intensity was increased. A maximum photocurrent of about 300 μ A and a maximum photo-voltage of about 0.6 V were produced for a light intensity of 5mW/cm² using poly(β -pinene) polymer whereas maximum photocurrent of about 250 μ A and a maximum photo-voltage of about 0.75 V were produced for same light intensity using cis-polyisoprene polymer. These measurements show highly promising results for the application in low cost photo-detectors and photo-sensors when compared to traditional photo-detectors. Additional applications will include low cost solar cells.

In the future, further work needs to be done to produce the photovoltaic cells with thickness in the range of a few nanometers, to enhance the current produced. Also, work needs to be done in the area of current and efficiency measurements. To increase the efficiency, we can even try to encapsulate the cell fabricated which may result in increase in lifetime.

It was recorded that the optical absorption of undoped cis-polyisoprene to be clearly transparent but at low doping it shows two peaks, one due to formation of cation radicals at

$\sim 4.27\text{eV}$ and second due to charge transfer between double bond and dopants (electron acceptors) at $\sim 3.3\text{eV}$. The concentration of these radicals increases approximately linearly with dopant concentration until saturation. Modulation depth of 5% was observed for the very first time for an applied field of $1\text{ V}/\mu\text{m}$ for a $50\mu\text{m}$ thick film, which is much higher than the modulation depth of other non-conjugated polymers till date. Exceptionally large Kerr coefficient as measured $1.6 \times 10^{-10}\text{ m/V}^2$ are exceptionally large and have been attributed to the subnanometer size metallic domains (quantum dots) formed upon doping and charge transfer.

For the very first time quadratic electro-optic effect has been observed in a waveguide when ac field is applied. The throughput of the waveguide was 5% involving iodine doped nonconjugated conductive polymer. The modulation depth observed for this waveguide was 1% for an applied field of $0.3\text{ V}/\mu\text{m}$. These initial results look very promising. The modulation depth in waveguide can be improved by initially improving the throughput. Also by increasing the thickness of doped polymer formed across the cladding layer so that applied electric field passes completely through the doped region.

Bibliography

1. M. Thakur, "A class of conducting polymers having nonconjugated backbones" *Macromolecules*, 21 (3), pp 661–664, 1988; M. Thakur and B.S. Elman, "Optical and magnetic properties of a nonconjugated conducting polymer". *J. Chem. Phys.* **1989**, 90, 2042.
2. M. Thakur, "Nonconjugated conductive polymer" *J. Macromol. Sci., Pure Appl. Chem.*, A38 1337, 2001.
3. M. Thakur, R. Swamy. and J. Titus, "Quadratic Electrooptic Effect in a Nonconjugated Conductive Polymer" *Macromolecules*, 37 (8), pp 2677–2678, 2004.
4. D.V.G.L.N. Roa, P.Wu, B.R. Kimball, M. Nakashima, B.S. Decristofano, "Trends in Optics and Photonics", 63, WB4/1- WB4/3, 2001.
5. G. P. Agrawal and R. W. Boyd. Contemporary Nonlinear Optics", *Academic Press*, 1992.
6. Jerry I. Dadap, Jie Shan, and Tony F. Heinz, "Theory of optical second-harmonic generation from a sphere of centrosymmetric material: small-particle limit", *JOSA B*, Vol. 21, Issue 7, pp. 1328-1347, 2004
7. Y L. Fletcher, M.A., F.R.S London, "The Optical Indicatrix and the Transmission of Light in Crystals", *Henry Fkowde, Oxford University Press Ware house, Amen Corner*, 1892.
8. M. Samoc, A. Samoc, B. Luther-Davis, Z. Bao, L. Yu, B. Hsieh, U. Scherf, *J. Opt. Soc. Am. B* 15 (1998) 817.
9. P.N. Prasad, D.J. Williams, Introduction to Nonlinear Optical Effects in Molecules and Polymers, John Wiley & Sons, Newyork, 1991.
10. R.W. Munn, C.N. Ironside, Principles and Applications of Nonlinear Optical Materials, Blackie Academic & Professional, USA, 1993.
11. J.M. Ballesteros, R. Serna, J. Solis, C.N. Afonso, A.K. Petford-Long, D.H. Osborne, R.F. Haglund Jr., *Appl. Phys. Lett.* 71 (1997) 2445.
12. R. W. Boyd. Nonlinear Optics. Academic Press, 2003.
13. Y R Shen. The Principles of Nonlinear Optics. John Wiley and Sons, Newyork, 1984.
14. E G Sauter. Nonlinear optics. Wiley-Interscience, 1996.

15. A Yariv and P Yeh. Optical waves in crystals. Wiley New York, 1984.
16. G. P. Agrawal and R. W. Boyd, "Contemporary Nonlinear Optics", Academic Press, 1992.
17. R Paschotta. Encyclopedia of laser physics and technology. Vch Pub, 2008.
18. H S Nalwa and S Miyata. Nonlinear optics of organic molecules and polymers. CRC press, 1997.
19. Ananthakrishnan Narayanan "Electrical and Nonlinear Optical Studies of Specific Organic Molecular and Nonconjugated Conductive Polymeric Systems."
20. P Weinberger. Philosophical Magazine Letters, 8(12): 897–907, 2008
21. Alfa Aesar "Nonlinear Optical Materials"
22. L. R. Dalton, et.al., Chem. Mater., 1995, 7, 1060
23. (a) F. Pan, et.al., Appl. Phys. Lett., 1999, 74, 492; (b) T. Kaino, et.al., Adv. Funct. Mater. , 2002, 12, 599; (c) W. Geis, et.al., Appl. Phys. Lett., 2004, 84, 3729; (d) F. Pan, et.al. , Appl. Phys. Lett., 1996, 69, 13; (e) U. Meier, et.al., J. Appl. Phys., 1998, 83, 3486.
24. (a) L. R. Dalton, Pure Appl. Chem., 2004, 76, 1421. Y. Shi, et.al., Science, 2000, 288, 119; (b) L. R. Dalton, et.al., Adv. Mater., 2002, 14, 1339.
25. P A Franken; A E Hill; C W Peters; G Weinreich. Phys. Rev. Lett., 7: 118, 1961.
26. P D Marker; R W Terhune; M Nisenoff; C M Savage. Phys. Rev. Lett., 8: 21, 1962.
27. J A Giordmaine. Phys. Rev. Lett., 8: 19, 1962.
28. G D Boyd; C K N Patel. Appl. Phys. Lett., 5: 234, 1964.
29. P M Rentzepis; Y H Pao. Appl. Phys. Lett., 5: 156, 1964.
30. G H Heilmair; N Ockman; R Braunstein; D A Kramer. Appl. Phys. Lett., 5: 229, 1964.
31. Ch Bosshard; K Sutter; P Pretre; J Hulliger; M Florsheimer; P Kaatz; P Gunter. Advances In Nonlinear Optics. Gordon and Breach Publishers, 1995.
32. Fritts C, Proc. Am. Assoc. Adv. Sci. , 33, (1883), pp. 97
33. ORGANIC SOLAR CELLS Tom J. Savenije, DelftChemTech, Faculty of Applied Sciences, Delft University of Technology
34. Comparing organic to inorganic photovoltaic cells: Theory, experiment, and simulation Brian A. Gregg and Mark C. Hanna.

35. Jitto Titus “Studies of the off-resonant nonlinear optical properties of an organic molecular crystal and specific nonconjugative polymers “.
36. Hideki Shirakawa, Edwin J. Louis, et. Al, “Synthesis of Electrically conductive organic Polymers: Halogens Derivatives of Polyacetylene,(CH) X ” *J.S.C Chem. Comm.*, 578 –580, 1977
37. H Rajagopalan; P Vippra; M Thakur. *Appl. Phys. Lett.*, 88: 033109/1, 2006.
38. Guo-Qing Yu and M. Thakur, “Electrical Conduction in Nonconjugated polymer doped with SnCl₄ and SbCl₅”, *Journal of polymer science: Part B*, Vol. 32, 2099-2104,(1994)
39. Jerry I. Dadap, Jie Shan, and Tony F. Heinz, “Theory of optical second-harmonic generation from a sphere of centrosymmetric material: small-particle limit”, *JOSA B*, Vol. 21, Issue 7, pp. 1328-1347, 2004
40. P. Vippra, H. Rajagopalan, M. Thakur, “Electrical and Optical Properties of a Novel Nonconjugated Conductive Polymer, Poly(β -pinene)”, *J Polym. Sci. Part B: Polym. Phys.* 43: 3695–3698, 2005.
41. A. Narayanan and M. Thakur, *Solid State Comm.*, 150, 375, 2010.
42. S. Shrivastava, and M. Thakur “Quadratic electro-optic effect in the nonconjugated conductive polymer iodine-doped trans-polyisoprene, an organic nanometallic system”, *Solid State Communication*, 2011.
43. Mark S. M. Alger, *Polymer Science Dictionary*
44. U.S. Census Bureau, *International Data Base*, 2008 First Update
45. History: Energy Information Administration (EIA), *International Energy Annual 2004* (May-July 2006)
46. Projections: EIA, *System for the Analysis of Global Energy Markets* (2007)
47. World Consumption of Primary Energy by Energy Type and Selected Country Groups, 1980-2004. Energy Information Administration, U.S. Department of Energy (July 31, 2006). Retrieved on 2007-01-20.
48. BP Statistical review of world energy June 2006. British Petroleum (June 2006). Retrieved on 2007-04-03
49. Renewables, *Global Status Report 2006*. Renewable Energy Policy Network for the 21st Century (2006). Retrieved on 2007-04-03
50. R. Swamy, H. Rajagopalan, P. Vippra, M. Thakur, A. Sen, *Solid State Communications*, Volume 143, Issues 11–12, September 2007, Pages 519-521

51. G. Nimitz, A. Enders, P. Marquardt, R. Pelster and B. Wessling, *Synth. Met.*, 45 (1991)197.